UNIVERSITY OF CALIFORNIA

Santa Barbara

A chemical genetics approach to study the Integrated Stress Response reveals common and new signaling mechanisms

A dissertation submitted in partial satisfaction of the requirements for the degree Doctor of Philosophy in Molecular, Cellular, and Developmental Biology

by

Nerea Muniozguren

Committee in charge:

Professor Diego Acosta-Alvear, Co-chair

Professor Brooke Gardner, Co-chair

Professor Meghan Morrisey

Professor Charles E. Samuel

September 2022

The dissertation of Nerea Muniozguren is approved.

_____

Meghan Morrisey

_____

Charles E. Samuel

_____

Brooke Gardner, Committee Co-Chair

_____

Diego Acosta-Alvear, Committee Co-Chair

August 2022

A chemical genetics approach to study the Integrated Stress Response reveals common and new signaling mechanisms

Nerea Muniozguren

To my mom and brother.

Without your love and support throughout these years,

I would not be writing this today. Thank you both for showing me

the true meaning of resiliency.

ACKNOWLEDGEMENTS

I want to thank everyone who helped me throughout my life and doctoral career with mentorship, scientific feedback, and friendship.

Ama Irene, Igor, Maitane, Izaro, Izar, Irati

Eskerrik asko (thank you) for your endless support and for providing the foundation that made it possible to pursue my interests. These achievements are as much yours as they are mine.

Diego Acosta-Alvear

Thank you, Diego. I am grateful to have done my doctorate research in your lab. Your mentorship and support throughout these years were essential to my research experience and life. You pushed me to think harder, strive harder and to be playful with science.

Francesca Zappa

Thank you for your endless support and patience during my pursuit of this research. Your scientific advice, help in planning experiments and willingness to answer all my scientific and non-scientific questions were so essential during this journey of mine. I am honored to have worked and learned from such a skilled scientist. I would not be where I am today without your help.

Brooke Gardner, Meghan Morrissey, and Charles E. Samuel

Thank you to my committee and additional faculty who have substantially contributed to my personal and academic growth while at UCSB. In particular to you Brooke, I am very grateful for you.

Ariadne Vlahakis

Your friendship and mentorship since I began working with you at UC Davis has been fundamental for my development as a researcher and as a person. You always pushed me to think critically and follow my dreams. You built me up when I struggled, and I so appreciate all of your support and friendship. You inspired me to earn my graduate studies in the United States, and for that I am grateful.

The Acosta-Alvear lab, The Arias lab, Incoming Graduate class of 2017, Marissa, Anthony and the MCDB department

To all the lab members, friends, mentors, helpers, and drinking buddies. None of this would have been possible or worth it without you all.

VITA OF NEREA MUNIOZGUREN

August 2022

EDUCATION

2017-2022 Ph.D. Molecular, Cellular, and Developmental Biology

University of California, Santa Barbara

2012-2013 M.S Molecular Biology and Biomedicine

University of the Basque Country (UPV/EHU)

2008-2012 B.S Biochemistry and Molecular Biology

University of the Basque Country (UPV/EHU)

RESEARCH EXPERIENCE

Aug. 2017-Present Ph.D. Candidate. University of California, Santa Barbara

Performed independent research focused on the molecular mechanisms controlling cellular stress responses.

Mar. 2015-Aug 2017 Research Scholar (J1 visa). University of California, Davis

-Performed independent research studying autophagy

-Discovered a novel role for TORC2 in mediating autophagy upon amino acid limitation

Jan. 2015-Mar. 2015 Junior specialist. Biophysics Unit (CSIC-UPV-EHU)

-Specialized in HIV study and vaccine design

Jan. 2014-Dec. 2014 Research Scholar (J1 visa). University of California, Davis

-Researched on autophagy

Sep. 2012-Jul. 2013 Master's thesis. University of the Basque country UPV/EHU

-Studied the effect of human LDL size in the cellular internalization

Sep. 2011-Jun. 2012 Bachelor's thesis. University of the Basque country UPV/EHU

-Studied membrane lipids and astaxanthin effect in the amyloid fibril formation

May 2010-Jun 2012 Undergraduate Assistant. University of the Basque country UPV/EHU

SCIENTIFIC PUBLICATIONS/CONTRIBUTIONS

-**Muniozguren NL**, Zappa F, Acosta-Alvear D (2022) The integrated stress response induces a common cell-autonomous death receptor 5-dependent apoptosis switch. bioRxiv 2022.07.04.498696; doi: https://doi.org/10.1101/2022.07.04.498696.

-Zappa F, **Muniozguren NL**, Wilson MZ, Costello MS, Ponce-Rojas JC, Acosta-Alvear D (2022) Signaling by the integrated stress response kinase PKR is fine-tuned by dynamic clustering. Journal of Cell Biology 221: e202111100.

-Vlahakis A, **Lopez Muniozguren N**, Powers T (2017) Msn2 and Msn4 couple TORC2-Ypk1 signaling and mitochondrial respiration to ATG8 gene expression and autophagy. Autophagy. 13(11):1804-1812. PMID: 29198169.

-Vlahakis A, **Lopez Muniozguren N**, Powers T (2017) Mitochondrial respiration links TOR complex 2 signaling to calcium regulation and autophagy. Autophagy.13(7):1256-1257. PMID: 28324658.

-Vlahakis A, **Lopez Muniozguren N**, Powers T (2016) Calcium channel regulator Mid1 links TORC2- mediated changes in mitochondrial respiration to autophagy. J Cell Biol. 215(6):779- 788. PMID: 27899413.

-Helped performing and contributed in the following paper (Acknowledgements):

Stauffer, B. and Powers, T. (2015) Target of rapamycin signaling mediates vacuolar fission caused by endoplasmic reticulum stress in *S. cerevisiae*. Mol. Bio. Cell

SCIENTIFIC CONFERENCES ASSISTED AND CONTRIBUTED TO

-Southern California RNA Meeting 2019. **Nerea L. Muniozguren**, Diego Acosta-Alvear. Pathway connectivity in the UPR and innate immunity

-ASCB 2018 Annual Meeting. **Nerea L. Muniozguren**, Diego Acosta-Alvear. Uncovering the cross-talk between the UPR and the innate immune pathways in response to double-stranded RNAs. P1687

-ASCB 2016 Annual Meeting. T. Powers, A. Vlahakis, **N.L. Muniozguren**. The rapamycin-insensitive TOR Complex 2 network signals through mitochondria and the ER to regulate autophagy during amino acid limited growth conditions. Microsymposium (Autophagy/ESCRT)

-XXII. IUBMB Congress Meeting (09/04-09/2012): Early effects of fish oil dietary intake on trout serum lipoproteins and muscle cholesterol deposition.

AWARDS AND FELLOWSHIPS

2019	Outstanding MCDB student award. UCSB
2019	Excellent poster presentation award. Southern California Meeting
2017-2018	Charles A. Storke Graduate Award. UCSB
2018	Doreen J. Putrah Cancer Research Foundation Conference Fellowship. UCSB
2017	International Doctoral Recruitment Fellowship (IDRF). UCSB
2012	Master’s student scholarship. The Basque Government

2012 Master's student scholarship. University of the Basque Country

2011 Undergraduate Research Assistantship. University of the Basque Country

TEACHING EXPERIENCE

2022 Teaching Assistant: General Biochemistry; Medical Immunology; General animal virology

2020-2021 Teaching Assistant: General animal virology; General genetics

2019 General animal Virology; General Biochemistry; Introductory Biology

2018 General animal virology

ABSTRACT

A chemical genetics approach to study the Integrated Stress Response reveals common and new signaling mechanisms

by

Nerea Muniozguren

Maintaining homeostasis is vital for biological systems. To maintain homeostasis, cells rely on specialized complex mechanisms, known as cell stress responses, that detect specific internal imbalances and react to them. The integrated stress response (ISR) is a fundamental signaling network that reprograms the transcriptome and proteome to leverage the cell's biosynthetic capacity against different stresses. Signaling plasticity is enabled by distinct ISR sensor kinases that detect specific perturbations. The ISR has two faces, with tailored homeostatic outputs and a terminal one engaged upon overwhelming stress. Through a chemical-genetics approach that uncouples natural stress inputs from ISR actuation, we show that the ISR engages a common, cell-autonomous apoptosis mechanism that requires unconventional signaling by death receptor 5. We also show that the ISR selectively activates the endoplasmic reticulum (ER) stress sensor IRE1 in the absence of ER stress. Together, our results indicate that a common ISR mechanism eliminates terminally injured cells and reveal a new level of intercommunication between the ISR and other stress responses.

TABLE OF CONTENTS

LIST OF FIGURES

LIST OF ABBREVIATION

ABL-2

Abelson-related proto-oncogene 2

ATF

Activating transcription factor

ASK1

Apoptosis signal-regulating kinase 1

BCL-XL

B-cell lymphoma-extra large

Bip

Binding immunoglobulin protein

BLOSC1S1

Biogenesis of lysosomal organelles complex1 subunit 1

C/EBP

CCAAT/enhancer-binding protein

CHOP

C/EBP homologous protein

Col6A1

Collagen type VI alpha 1 chain

DNAJB9

DnaJ heat shock protein family (Hsp40) member B8

DR5

Death receptor 5

FKBP

FK506-binding protein

GADD34

Growth arrest and DNA damage-inducible protein GADD34

GCN2

General control non-depressible protein 2

GM130

Golgi matrix protein 130

eIF2

Eukaryotic initiation factor 2

HEK 293

Human embryo kidney 293

HRI

Heme-regulated eIF2α kinase

IRE1

Inositol-requiring enzyme-1

IRES

Internal ribosome entry site

ISR

Integrated stress response

ISRIB

Integrated stress response inhibitor

JNK

c-Jun N-terminal kinases

KD

Knockdown

LD

Lumenal domain

NF-kB

Nuclear factor kappa light chain enhancer of activated B cells

PARP

Poly-ADP ribose polymerase

PCR

Polymerase chain reaction

PERK

PKR-like ER kinase

PKR

Double-stranded RNA-dependent protein kinase

PP1

Protein phosphatase 1

qRT-PCR

Real-time quantitative reverse transcription PCR

RIDD

Regulated IRE1 dependent decay

SCARA3

Scavenger receptor class A member 3

TNF

Tumor necrosis factor

TRAF

TNF receptor-associated factor 2

TRAIL

TNF-related apoptosis-inducing ligand

UPR

Unfolded protein response

U2OS

Human bone osteosarcoma cells

uORFs

Upstream regulatory open reading frames

XBP1

X-box binding protein 1

CHAPTER 1. Introduction

Homeostasis and Cellular Stress Responses

Maintaining homeostasis is vital for biological systems. Homeostasis ensures the stability of biological systems by preserving internal composition and allowing the cell/organism to function properly as changes occur in the internal or external environment (Buchman, 2002). Organisms operate in relatively narrow set of conditions and, therefore, it is crucial to regulate the concentrations and properties of cellular building blocks to ensure cell survival. Indeed, disruption of homeostasis contributes to disease progression (Galluzzi et al, 2018; Fuchs & Steller, 2015). Consequentially, mechanisms that control and regulate cell homeostasis are fundamental for organismal fitness and survival. Different types of stress can tax cell physiology in different ways, and thus, cells rely on different stress responses that are tasked with restoring and maintaining homeostasis under specific circumstances.

Stress responses have at least three interdependent components: (1) A sensor or receptor that detects changes in the internal or external environment, (2) the integrating center or control center that receives information from the sensors and passes on the information to downstream effectors, and (3) effectors that interpret information passed by the control center to initiate regulatory programs that restore homeostasis, such as the induction of gene expression programs (Fig. 1). The cell's initial response to a perturbation prepares the cell to defend against and recover from the insult. However, if the noxious stimulus is unresolved, cells from multicellular organisms activate death signaling pathways that sacrifice the cell to preserve the organism. Two fundamental stress responses are the integrated stress response

(ISR) and the unfolded protein response (UPR). The ISR and UPR are interconnected signaling networks governed by sensors that detect multiple stress inputs, ranging from nutritional deficits, oxidative stress, mitochondrial dysfunction, aberrant RNA accumulation, to unfolded proteins in the endoplasmic reticulum (Pakos-Zebrucka et al, 2016; Fulda et al, 2010). The ISR operates by reprogramming transcription and translation, passing information about encounters with different stress inputs through a central relay, the master translation initiation factor eukaryotic initiation factor 2 (eIF2), to control general translation initiation rates and induce specific effectors. The UPR, on the other hand, detects protein-folding perturbations in the lumen of endoplasmic reticulum (ER) (Costa-Mattioli & Walter, 2020; Hetz, 2012).

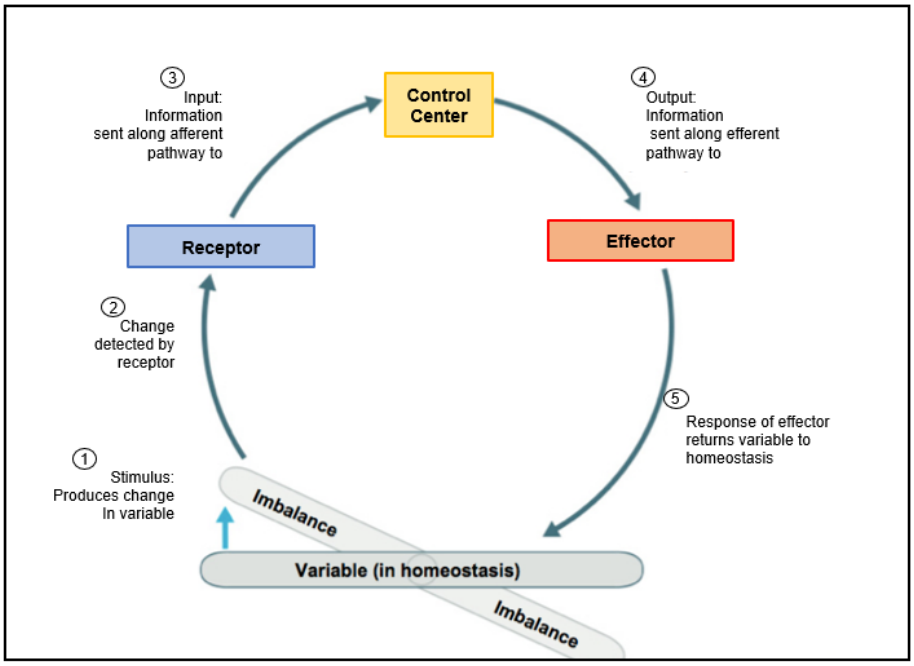

Figure 1. Homeostasis control. Homeostasis is a property of human biological systems where the self-regulating systems preserve the balance for cell/organism survival by circulating information through the receptor to the effector(s) (modified from Khan, 2021).

The Integrated Stress Response

The ISR is an evolutionarily conserved intracellular signaling network that helps the cell, tissue, and organism adapt to a variable environment. In response to different environmental and pathological conditions, including protein homeostasis (proteostasis) defects, nutrient deprivation, viral infection, and oxidative stress, the ISR restores homeostasis by reprogramming the proteome and controlling comprehensive gene expression programs (Fig. 2).

The ISR is governed by four sensor kinases, GCN2, HRI, PKR, and PERK, all of which possess functionally homologous kinase domains, but distinct regulatory domains (Harding et al, 1999; Berlanga et al, 1998, Chen et al, 1991; Meurs et al, 1990; Ramirez et al, 1991). As such, each sensor kinase responds to distinct and specific stress inputs while converging on the phosphorylation of a single serine residue-Ser51-in the alpha subunit of the eukaryotic initiation factor 2 (eIF2α) (Reviewed in Costa-Mattioli & Walter, 2020). The localization of the kinases could confer subcellular specificity to the ISR, as HRI, PKR, and GCN2 are localized to the cytosol, while PERK is localized to the ER membrane (Costa-Mattioli & Walter, 2020).

GCN2 (general control nonderepressible 2) is highly conserved from yeast to humans. Although GCN2 is expressed broadly among tissues, its expression is particularly high in the brain and liver (English et al, 2021). Mechanistic insights into GCN2 regulation indicate that amino acid deprivation activates GCN2 via a mechanism that may occur by sensing uncharged tRNAs, or ribosome stalling and ribosome collisions (Vazquez de Aldana et al 1994; Inglis et al, 2019), making GCN2 a sensor of translation defects. In addition to amino acids deprivation, GCN2 can also

be activated by UV irradiation, hydrogen peroxide, heat shock, and osmotic shock (Castilho et al, 2014; Deng et al 2002).

HRI (heme-regulated inhibitor) is primarily expressed in erythroid cells (Han et al, 2001; Chen, 2014). HRI contains two kinase domains and two heme-binding sites that respond to cellular heme levels (Rafie-Kolpin et al, 2000). HRI is activated in the absence of heme, and regulates hemoglobin synthesis depending on the heme availability (Han et al, 2001). Other stressors that can also activate HRI include heat shock, arsenite-induced oxidative stress, nitric oxide, osmotic stress and 26S proteasome inhibition (Ill-Raga et al, 2015; McEwen et al, 2005; Yerlikaya et al, 2008; Guo et al 2020).

PKR (double-stranded RNA-dependent protein kinase) is activated mainly by double-stranded RNA (dsRNA) (Lemaire et al, 2008) produced during viral infection to prevent viral gene expression (Eiermann et al, 2020). In addition to its kinase domain, PKR contains two N-terminal double-stranded RNA-binding motifs (Sadler & Williams, 2007). Upon detection of dsRNA, PKR is activated by dimerization (Wu 7& Kaufman, 1997; Vattem et al, 2001) followed by the formation of dynamic clusters (Zappa et al, 2022). Although PKR is activated by dsRNA that is often of viral origin, it can also be activated by endogenous dsRNA in the absence of viral infection by stimuli such as mitochondrial dsRNA (Kim et al, 2018), dsRNA arising from Alu repeats (Elbarbary et al, 2013), or the viral dsRNA synthetic mimic poly I:C (Zappa et al, 2022). Interestingly, PKR has been shown to be activated by other stresses in a dsRNA-independent manner including oxidative and ER stress, growth factor

deprivation, cytokine or bacterial infection, and stress granules (Li et al, 2006; Guo et al, 2019; Gal-Ben-Ari et al, 2019).

PERK (PKR-like ER kinase), found in metazoans, is a transmembrane protein located in the ER membrane that is also part of the UPR. The C terminus of PERK faces the cytosol and includes its kinase domain, and the N terminus sensor domain lies within the ER lumen (Marciniak et al, 2006). Upon detection of unfolded proteins in the ER, PERK oligomerizes and is auto-phosphorylated in the plane of the ER membrane (Harding et al, 1999). Other stressors such as UV light (Wu et al, 2002), and heat shock (Li et al, 2014), can also activate PERK.

All ISR kinases converge on phosphorylating a single serine in the alpha subunit of the eukaryotic initiation factor 2 (eIF2α), a heterotrimeric GTPase that, together with GTP and the initiator methionyl tRNA, forms the ternary complex which is required to initiate translation. Phosphorylated eIF2α acts as a competitive inhibitor of its guanine nucleotide exchange factor eIF2B (Adomavicius et al, 2019; Schoof et al, 2021), and as such, it decreases the availability of ternary complex leading to a global shutdown of protein synthesis. However, some mRNAs harboring upstream regulatory open reading frames (uORFs) escape this regulatory control and are selectively translated upon eIF2α phosphorylation. These mRNAs include those encoding the transcription factors ATF4 and CHOP, as well as *GADD34*, which encodes a regulatory subunit of protein phosphatase 1 (PP1) that dephosphorylates eIF2α and establishes a negative feedback loop that terminates ISR signaling (Novoa et al, 2003; Vattem & Wek, 2004; Hinnebusch et al, 2016). The gene expression changes driven by the ISR can either increase the biosynthetic capacity of the cell

downstream of ATF4 to restore homeostasis, or induce apoptosis downstream of CHOP if homeostasis cannot be restored.

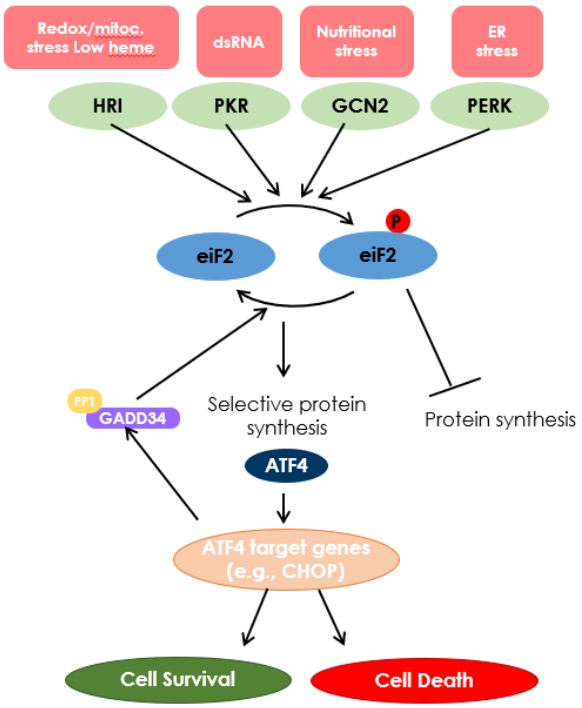

Figure 2. **The Integrated Stress Response pathway**. Heme depletion, mitochondrial stress, oxidative stress, dsRNA, nutritional stress, ER stress and translation defects (i.e., ribosome collisions) activate the ISR sensor kinases HRI, PKR, GCN2 and PERK, leading to the phosphorylation of eIF2α. eIF2α phosphorylation results in protein synthesis inhibition coupled to the selective translation of some mRNAs such as that encoding the transcription factor ATF4. ATF4 regulates the expression of genes that promote cellular adaption. Feedback control of the ISR is regulated by the holophosphatase GADD34-PP1, which dephosphorylates eIF2α to terminate the ISR (Modified from Tian et al, 2021).

The Unfolded Protein Response

The UPR is an evolutionarily conserved homeostatic mechanism that plays a critical role in monitoring the accumulation of misfolded proteins in the ER lumen and adjusts ER functions according to the cell's needs (Walter & Ron, 2011; Karagöz et al, 2019; Adams et al, 2019). The mammalian UPR consists of three signaling branches governed by three transmembrane ER stress sensor proteins: PERK, IRE1, and ATF6 (Fig. 3, Walter & Ron, 2011).

As mentioned above, PERK is a transmembrane kinase that is also a part of the ISR; by reducing global translation PERK is thought to protect the ER by reducing its protein folding load (Marciniak et al, 2006).

ATF6 is a membrane-tethered transcription factor that translocates to the Golgi apparatus upon ER stress where it is cleaved by the S1P and S2P proteases. This regulated proteolysis liberates ATF6's soluble transcription factor (ATF6-N), which translocates into the nucleus to induce ER biosynthetic and ER-associated protein degradation (ERAD) genes (Rutkowski & Hegde, 2010; Ye et al, 2000; C. Hetz, 2020). Although the precise mechanism of ATF6 activation is still unknown, there is evidence that suggests that ATF6 might be coupled to redox sensing (Nadanaka et al, 2007).

IRE1 is the most conserved of the three UPR sensors. It is a transmembrane kinase/endoRNase (Cox et al, 1993; Cox & Walter, 1996; Sidrauski and Walter, 1996) thought to detect unfolded proteins by direct binding to its ER lumenal sensor domain (Gardner & Walter, 2011; Karagöz et al, 2017). IRE1's activity is tuned by the abundant ER luminal chaperone BiP, which binds inactive monomeric IRE1 preventing further activation (Adams et al, 2019). Upon detection of unfolded proteins,

IRE1 oligomerizes, trans-autophosphorylates and activates its endoribonuclease activity. Active IRE1 coordinates the cytosolic splicing of the X-box-binding protein 1 (XBP1) mRNA to generate a potent transcription factor known as XBP1s (s refers to the spliced form) (Calfon et al, 2002). XBP1s upregulates genes that increase the cell's capacity for protein folding, protein degradation, and trafficking, which help to alleviate ER stress (Adam et al, 2019; Acosta-Alvear et al, 2007). XBP1s has also been associated with gene regulatory programs that are unrelated to processes associated with ER function, such as chromosomal architecture, cell growth and DNA replication and repair (Acosta-Alvear et al, 2007). IRE1 RNase activity can also lead to cleavage of ER-bound mRNAs in a process known as Regulated IRE1 Dependent Decay (RIDD) (Walter & Ron, 2011), which further helps to alleviate the burden of misfolded proteins in the ER.

Activation of IRE1 fundamentally depends on its oligomerization, which activates its cytosolic kinase and RNAse domains. While the accumulation of unfolded proteins in the ER lumen drives oligomerization of IRE1's lumenal domain, IRE1 can also sense changes in the ER membrane lipids and/or membrane composition, which is commonly referred to as lipid bilayer stress (Halbleib et al, 2017). Studies in yeast revealed that IRE1 senses membrane deformations through its transmembrane amphipathic helix (Halbleib et al, 2017). It is noteworthy that the transcription programs activated upon ER stress and lipid bilayer stress are different (Koh et al, 2018; Ho et al, 2020), suggesting specific IRE1-driven responses Therefore IRE1 is a good example of how one same node can face a delicate balance in response to

different stresses and induce a fine-tuned response, i.e., the activation of critical genes to adapt to specific stresses (Leber et al, 2004)

While IRE1 signaling pathway mediates protective responses through XBP1s and RIDD, active IRE1 has also been shown to recruit TNF receptor-associated factor 2 (TRAF2), which in turn recruits the apoptosis signal-regulating kinase (ASK1) (Nishitoh et al, 2002), to drive c-Jun amino-terminal kinase (JNK) activation and cell death (Urano et al, 2000). The cascade initiated by ASK1 leads to JNK activation and JNK activity activates the proapoptotic protein Bim (Lei & Davis, 2003), while inhibiting the antiapoptotic protein BCl-2 (Yamamoto et al, 1999) This IRE1 apoptotic pathway further demonstrates IRE1's ability to control cell fate in the face of ER stress.

While IRE1 and ATF6 responses are initially cyto-protective, unrelenting stress can also invoke UPR-driven apoptosis. The cellular outcome depends on a complex interplay of the signaling of the different branches of the UPR. During ER stress PERK induces the transcription factor CHOP downstream of ATF4 (Lu et al, 2014). CHOP induces the death receptor 5 (DR5) which drives apoptosis. However, IRE1 degrades the DR5 mRNA through RIDD, suppressing DR5 activation. When ER stress is unresolvable, IRE1 activity is attenuated, leading to accumulation of the DR5 mRNA and accumulation of DR5 protein. This mechanism is thought to constitute the UPR switch that drives apoptosis (Lu et al, 2014).

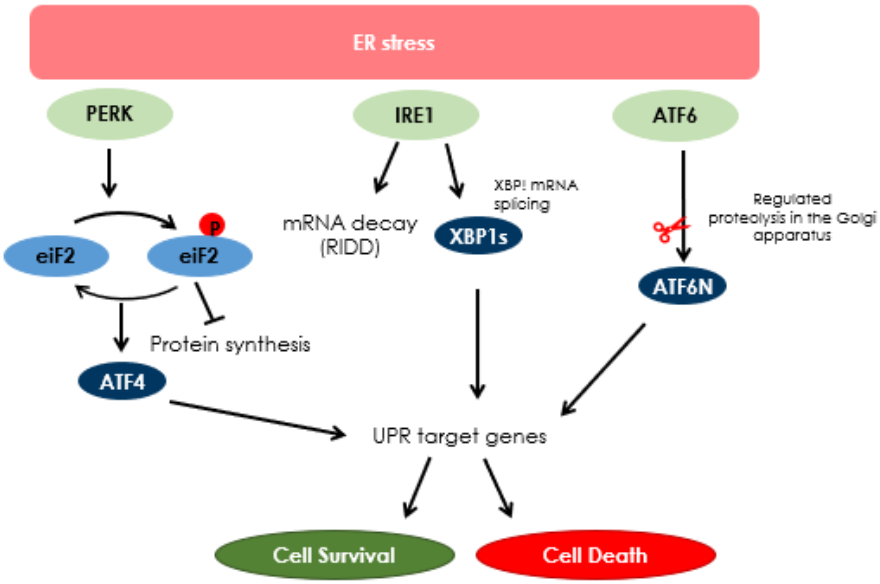

Figure 3. The Unfolded Protein Response. The UPR is governed by three ER stress sensors: IRE1, PERK and ATF6 that regulate comprehensive gene expression programs that lead to adaptation or cell death (Modified from Karagöz et al, 2019).

The importance of stress responses and open questions

Due to the ISR's fundamental role controlling survival or death, it is not surprising that its dysregulation is associated with numerous diseases, including Alzheimer's disease, Parkinson's disease, and Down Syndrome (Mouton-Liger et al, 2012; Ma et al, 2013; Hoozemans et al, 2007; Zhu et al, 2019). Therefore, therapeutic targeting of the ISR emerges as a promising avenue for treating such diseases.

A large body of work has revealed the intricacies of the ISR's molecular circuitry (reviewed in Costa-Matiolli & Walter, 2020). However, there are still gaps in our knowledge of ISR signaling. Many of the consequences downstream eIF2 phosphorylation are complex and remain poorly understood. For example, it is not yet understood how activation of downstream targets determine survival or death, or whether each branch of the ISR promotes the same cell death mechanism, or whether each stress input dictates a specific cell death pathway.

Stress signaling pathways do not signal in isolation, and accumulating evidence suggest a high degree of interconnectivity between them. For example, Zhu et al (2021) showed that the UPR can trigger the ISR through the cleavage of cellular RNAs. Despite evidence showing that these stress networks are interwoven, the molecular mechanisms that enable the cross-talk between the UPR and ISR are still not well-understood. A better understanding of the molecular mechanisms of the ISR would greatly facilitate approaches to modulate the ISR for therapeutic benefit. We address some of these questions in chapters 2 and 3.

In chapter 2, we demonstrate that the ISR uses a common mechanism that eliminates terminally injured cells, thereby preserving tissues and organs. In chapter

3 we discuss the interconnectivity of the ISR with the UPR. Our work thus demonstrates two new biological principles: (i) a universal ISR cell-autonomous apoptosis mechanism downstream of death receptor 5 to eliminate terminally injured cells, and (ii) interconnection between the ISR and the UPR via ISR-driven IRE1 activation in the absence of ER stress, linking the ISR and the UPR outside their shared node PERK.

CHAPTER 2

The integrated stress response induces a common cell-autonomous death receptor 5-dependent apoptosis switch

Note: Some figures, methods and discussion from this chapter have been previously published in ©Zappa et al (2022) and ©Muniozguren et al (2022).

Through activation of gene expression programs and translational control, the ISR reprograms the transcriptome and proteome to restore homeostasis. However, during persistent stress, the ISR can switch to drive apoptosis. Both outcomes, adaptation and cell death, protect the organism by preserving healthy cells and eliminating terminally damaged ones. Signaling dynamics and intercommunication between nodes could explain the dichotomy between an adaptive and a terminal ISR. Indeed, during ER stress, opposing signals between PERK and the evolutionarily conserved ER stress sensor kinase/RNase IRE1 dictate adaptive or terminal outcomes (Lu et al, 2014). In response to ER stress, PERK induces CHOP, which in turn induces Death Receptor 5 (DR5), a transmembrane receptor belonging to the Tumor Necrosis Factor (TNF) superfamily of death receptors together with DR4, TNF, and Fas (Yamaguchi & Wang, 2004). Ligand binding promotes self-association of DR5 and recruitment of the adaptor protein FADD and procaspase-8 to nucleate the Death-Inducing Signaling Complex (DISC), which processes procaspase-8 into active caspase-8 (Wilson et al, 2009). In the early, adaptive phase of the ER stress response, IRE1 cleaves the DR5 mRNA, which leads to its degradation. Dampening of pro-

survival IRE1 signaling during persistent ER stress switches the balance in favor of pro-apoptotic signaling downstream of the PERK-CHOP axis, which results in accumulation and activation of DR5. Notably, in this mechanism, DR5 accumulates in the *cis*-Golgi apparatus and signals unconventionally, in a ligand-independent manner, to engage a cell-autonomous death program (Lu et al, 2014; Lam et al, 2020).

Prompted by these observations, in this chapter we have addressed whether the ISR as a whole—and not PERK alone—engages a universal cell-autonomous apoptosis program dependent on unconventional DR5 signaling.

Different ISR inputs induce DR5 and apoptosis

To dissect whether terminal ISR signals downstream of different stress inputs converge on DR5 expression, we treated H4 neuroglioma cells with various stressors that activate each of the ISR kinases. We chose a neural cell line because a dysregulated ISR has been observed in numerous neuropathologies (Costa-Mattioli & Walter, 2020). To induce ER stress and activate PERK, we treated cells with the ER calcium reuptake inhibitor thapsigargin (Schröder, 2008; Oslowski & Urano, 2011). To induce dsRNA stress and activate PKR, we transfected cells with the dsRNA mimetic polyinosinic-polycytidylic acid (poly I:C) (Balachandran et al, 2000). To induce mitochondrial stress and activate HRI, we treated cells with the ATP synthase inhibitor oligomycin (Guo et al, 2020). Finally, to mimic nutritional deficit and activate GCN2, we treated cells with histidinol, a histidine analog alcohol that prevents histidyl-tRNA charging (Harding et al, 2019). We next measured the levels of DR5 mRNA by qRT-

PCR upon exposure of the cells to the abovementioned stressors for 18 hours, which we reasoned would be sufficient to initiate a terminal response based on previous observations (Lu et al, 2014) (Fig. 4A). This analysis revealed an approximately 4-fold upregulation of the DR5 mRNA in response to ER stress elicited by thapsigargin (Fig. 4A), consistent with the upregulation of DR5 mRNA observed in colon cancer cells subjected to persistent ER stress (Yamaguchi & Wang, 2004). Poly I:C, oligomycin, and histidinol also elevated the levels of the DR5 mRNA, albeit less potently, with approximately 2-fold (poly I:C and oligomycin) to 3-fold (histidinol) increases. Notably, we did not detect the mRNA encoding the death receptor DR4, which encodes a protein related to DR5 (Wilson et al, 2009) (Fig.S4A).

The increase in DR5 mRNA elicited by any of the stressors we used was reflected at the protein level, with induction of both the long (DR5L) and short (DR5S) isoforms (DR5L, ranging from approximately 3.5- to 4.5-fold upregulation) (Valley et al, 2012) (Fig. 4B,C). The stress-induced upregulation of DR5 isoforms was accompanied by the processing of procaspase-8, activation of caspase-3, and cleavage of the canonical apoptosis marker PARP1 (Fig. 4B), which is consistent with DR5's pro-apoptotic activity. Expectedly, these changes tracked with activation of the ISR, as indicated by phosphorylation of the ISR sensor kinases and eIF2α, as well as induction of ATF4 and CHOP (Fig. 4B; S4B).

Given that DR5 is induced by CHOP (Yamaguchi & Wang, 2004), our results suggest that the cell death decision is relayed to terminal effectors by eIF2α phosphorylation—the ISR core. If this is the case, inhibition of the ISR should suppress DR5 accumulation and apoptosis. To test this possibility, we co-treated cells

with the small molecule ISR inhibitor ISRIB, which renders cells less sensitive to the effects of eIF2α phosphorylation (Sidrauski et al, 2015) and the different ISR stressors aforementioned. ISRIB inhibited the upregulation of DR5 mRNA (Fig. 4D), and it restored cell viability, measured by the exclusion of the cell-impermeable DNA dye propidium iodide (PI) in live cells (Fig. 4E). These results indicate that cell-death signals can be bypassed in cells that are refractory to the effects of phosphorylated eIF2α and substantiate the notion that the ISR core passes the cell death decision to terminal effectors.

We next examined the ability of phosphorylated eIF2α to induce DR5 without any of the stress-inducing agents we used. To this end, we employed a genetics-based approach in which we force-expressed eIF2α^{S51D}, a phosphomimetic point mutant of eIF2α, under the control of a tetracycline-regulatable promoter. Induction of eIF2α^{S51D} in H4 cells treated with doxycycline revealed a time-dependent accumulation of DR5 mRNA, starting at 8 hours after induction and reaching saturation at 16 hours (Fig. 4F). This time frame is consistent with the expression of the eIF2α^{S51D} and consequent activation of the ISR (Figs. S4C-E). Furthermore, the upregulation of DR5 mRNA was mirrored by DR5L and DR5S proteins (average 3-fold induction at 16 hours for DR5L) (Figs. 4G, H). Together, these results indicate that DR5 is induced by the different branches of the ISR downstream of phosphorylated eIF2α.

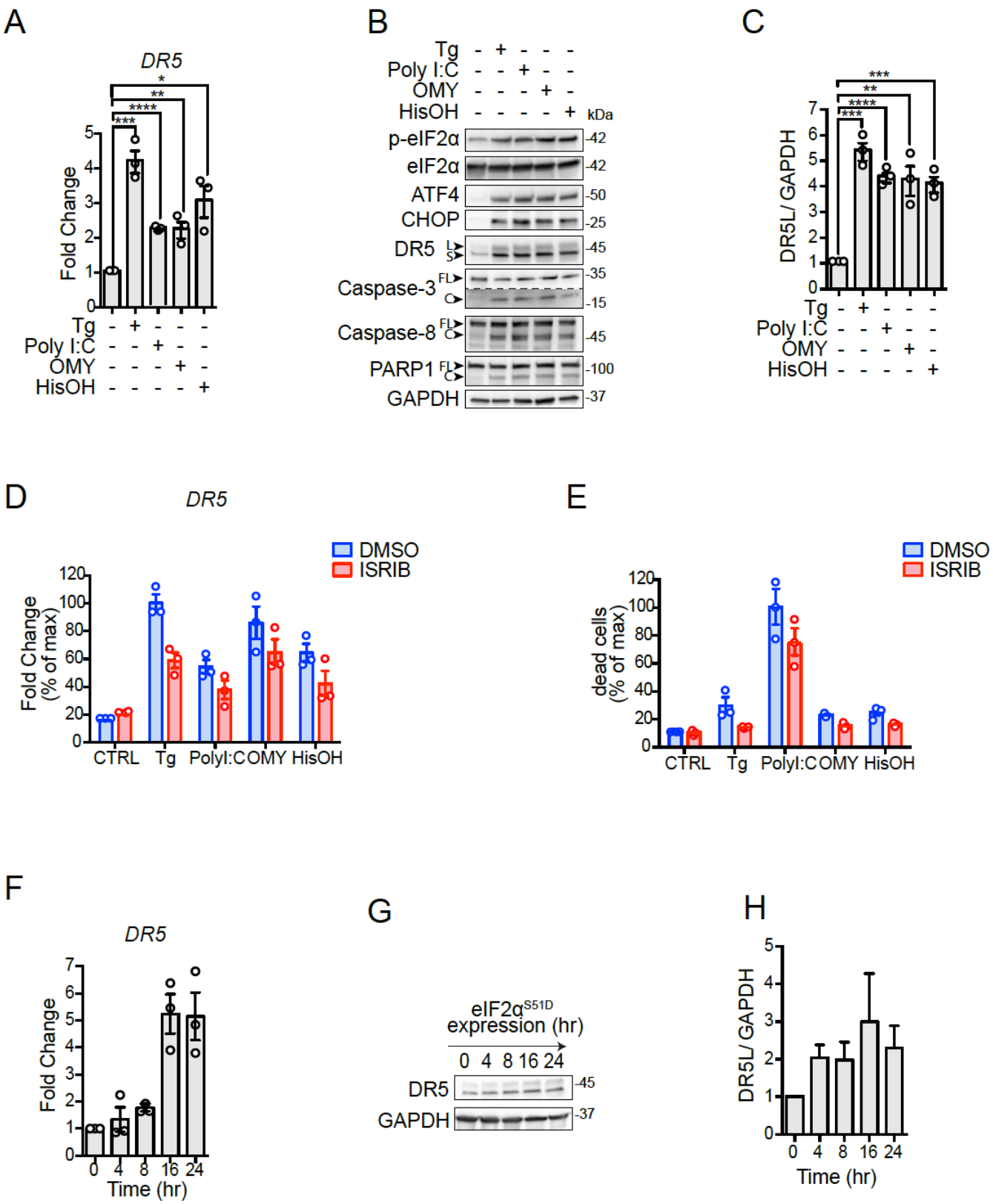
A
DR5
Fold Change
Tg
Poly I:C
OMY
HisOH
B
Tg
Poly I:C
OMY
HisOH
kDa
p-eIF2α
eIF2α
ATF4
CHOP
DR5
Caspase-3
Caspase-8
PARP1
GAPDH
C
DR5L/GAPDH
D
DR5
DMSO
ISRIB
Fold Change (% of max)
CTRL
Tg
PolyI:C
OMY
HisOH
E
DMSO
ISRIB
dead cells (% of max)
F
DR5
Fold Change
Time (hr)
G
eIF2α^S51D expression (hr)
DR5
GAPDH
H
DR5L/GAPDH
Time (hr)

Figure 4. **Activation of different branches of ISR induces DR5 and cell death.** (A) Quantitative real-time PCR analysis of DR5 mRNA levels in H4 cells after activation of different branches of the ISR. Thapsigargin (Tg) 300 nM, poly I:C 250 ng/ml, oligomycin (OMY) 3 µM, histidinol (HisOH) 5 mM (mean and SEM, N = 3, ****P < 0.0001, ***P < 0.001, **P < 0.01, *P < 0.05 unpaired Student's t-test, non-parametric). (B) Western blot showing upregulation of DR5, cleavage of caspase-8, caspase-3, and PARP1, and induction of canonical ISR markers (p-eIF2α, ATF4 and CHOP) in H4 cells upon treatment with different ISR stressors for 18 hours. GAPDH: loading control. (C) Densitometry quantification of the Western blot data for DR5 long isoforms (mean and SEM, N = 3, ****P < 0.0001, ***P < 0.001, **P < 0.01 unpaired Student's t-test, non-parametric). (D) qRT-PCR analysis of DR5 mRNA levels after pre-treating H4 cells with the ISR inhibitor ISRIB (mean and SEM, N = 3, ****P < 0.0001 One-way ANOVA). (E) Quantification of cell viability analysis using flow cytometry after staining with propidium iodide. The plot shows the induction of cell death in H4 cells upon treatment with classical pharmacological ISR activators and the restoration of cell viability upon ISR inhibition using ISRIB. Data are expressed as a percentage of the maximum value (mean and SEM, N = 3, ****P < 0.0001 One-way ANOVA). (F) qRT-PCR analysis of DR5 mRNA levels in H4 cells expressing eIF2α^{S51D} (mean and SEM, N = 3, ***P < 0.001 One-way ANOVA). (G) Western blot showing upregulation of DR5 isoforms in H4 cells after activation of eIF2α^{S51D}. GAPDH: loading control. (H) Densitometry quantification of the Western blot data for DR5 long isoform. GAPDH: loading control.

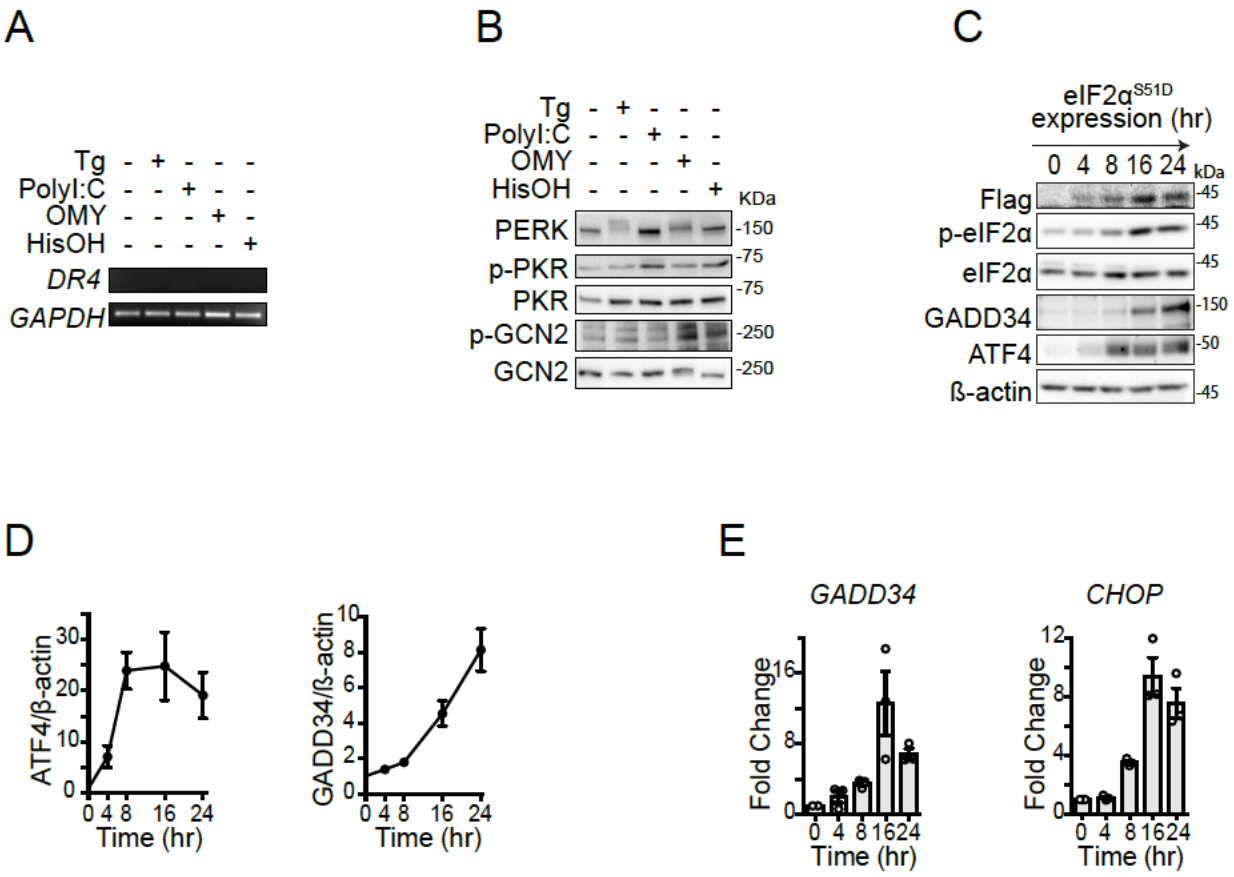

Figure S4. Pharmacological and genetic ISR induction in H4 cells. (A) Analysis of DR4 mRNA levels by RT-PCR in H4 cells after activation of the ISR with different pharmacological agents shows undetectable levels of DR4 transcript. GAPDH: loading control. Thapsigargin (Tg) 300 nM, poly I:C 250 ng/ml, oligomycin (OMY) 3 µM, histidinol (HisOH) 5 mM. (B) Western blot showing phosphorylation of the ISR sensor kinases in H4 cells upon treatment with pharmacological ISR inducers. (C) Western blot showing canonical ISR induction in H4 cells expressing FLAG epitope-tagged eIF2α^{S51D} and treated with doxycycline for the indicated time. β-actin: loading control. (D) Densitometry quantification of the Western blot data in (C) for ATF4 and GADD34 (mean and SEM, N = 3). (E) qRT-PCR analysis of ATF4 and CHOP mRNA levels in H4 cells expressing FLAG epitope-tagged eIF2α^{S51D} and treated with doxycycline for the indicated time (mean and SEM, N = 3).

A synthetic biology approach to control the ISR

1. A problem with natural inputs and linear pathway activation

Traditional approaches to study the ISR rely on the exposure of cells or animal models to drugs (dsRNA mimics, ER and mitochondrial poisons), physical agents (UV-light) or nutrients withdrawal (amino acid starvation) (reviewed in Pakos-Zebrucka et al, 2016). Although powerful, these methods have the limitation to simultaneously activate multiple stress response pathways, thus making it harder to dissect the molecular and gene signature that are under the exclusive control of the ISR. For instance, thapsigargin activates the ISR and the UPR at the same time (Elouil et al, 2007), and poly I:C promotes a simultaneous activation of multiple dsRNA binding proteins such as Toll-like receptor 3 and MDA-5 (McCartney et al, 2009; Pichlmair et al, 2009; Zhou et al, 2014).

Other main strategies to study the individual roles of ISR kinases rely on blocking its activity through RNA interference (RNAi)-based approaches and/or generating true knockouts. However, these strategies could give rise to several problems that could obscure our results. First, targeting ISR kinases by RNAi is challenging because of the high degree of relatedness among eIF2α kinases (~27% identity; ~45% similarity at nucleotide level) (Taniuchi et al, 2016). Second, RNAi-based approaches could overwhelm the cell's microRNA processing machineries (Grim, 2011). Third, knockout cells could still express truncated proteins (Baltzis et al, 2002).

While powerful the use of the eIF2α^{S51D}, under the control of a tetracycline-regulatable promoter, to activate ISR downstream eIF2α, it is important to point out that the phosphomimetic proteins are overexpressed in cells, which exhausts the resources of the cell to make and transport proteins, and could result in detrimental effects on cellular functions (Stoebel et al 2008).

For these reasons, we bypassed these limitations by using a chemical-genetic approach to study the “pure ISR” activation in living cells, allowing us to isolate and precisely define signaling events downstream eIF2α, without the confounding effects of the simultaneous activation of multiple stress sensors.

2. A chemical genetics approach allows ISR activation through precise input control

To dissect the molecular circuitry exclusive to the terminal ISR and avoid the pleiotropic effects of stress-inducing agents, we employed a chemical-genetics approach consisting of an engineered ISR sensor kinase, FKBP-PKR, which can be activated with a small molecule ligand to induce the canonical ISR (Zappa et al, 2022). Unlike the classical ISR stress-inducing agents mentioned above, FKBP-PKR allows a precise, stress-free activation of a “pure” ISR. We chose to engineer PKR for several reasons; First, PKR is a cytosolic soluble protein (reviewed in William, 1999). Second, the structural composition of PKR is well characterized (Sadler & Williams, 2007). Third, PKR’s mechanism of activation by dimerization is well described in the literature (Dey et al, 2005; Dar et al, 2005; Lemaire et al, 2015).

To this end, we replaced the dsRNA sensor domain of PKR with a bump-and-hole mutation (F36V) of the immunophilin FK506-binding protein (FKBP) that allows its dimerization with small drug-like molecule (homodimerizer, the synthetic bivalent ligand AP20187) (Clackson et al, 1998; Yang et al, 2000) (Fig. 5A), and does not affect endogenous FKBP (referred henceforth as FKBP-PKR). We FLAG-epitope tagged FKBP-PKR and introduced it into a retroviral expression vector that simultaneously expresses GFP from an internal ribosomal entry site (IRES) (Fig. S5A). To eliminate any contribution to the signaling of the endogenous PKR, we introduced this vector in the H4 PKR knockdown stable cell line we generated by genetically silencing endogenous PKR by CRISPR interference (CRISPRi) with a very high (> 99%) efficiency in H4 cells (Fig. S5B). These H4 cells stably express a catalytically-dead Cas9 nuclease (dCas9) fused to a trans-repressor domain. Co-expression of short guide RNAs targeting PKR's gene promoters allowed us to efficiently inhibit its gene expression. CRISPRi is a well-established technology (Gilbert et al, 2013) that allows transcriptional silencing which without the aforementioned problems associated with RNAi or true knockouts.

We selected a sub-clonal population of FKBP-PKR cells based on GFP levels using fluorescence activated cell-sorting (FACS) and we analyzed the ISR signaling of FKBP-PKR cells treated with the homodimerizer. Autophosphorylation of FKBP-PKR and the consequent phosphorylation of eIF2α occurred by 5 minutes after treatment and exponentially increased during 60 minutes of stimulation (Fig. 5B). In line with this observation, global translation, measured by the ability of cells to

incorporate puromycin into nascent polypeptides, was almost completely arrested after 60 minutes of FKBP-PKR activation (Fig. 5C).

Time-course analysis of cells treated with the homodimerizer for 24 hours demonstrated induction of canonical ISR molecular changes, including induction of ATF4, GADD34 and CHOP (Fig. 5D).

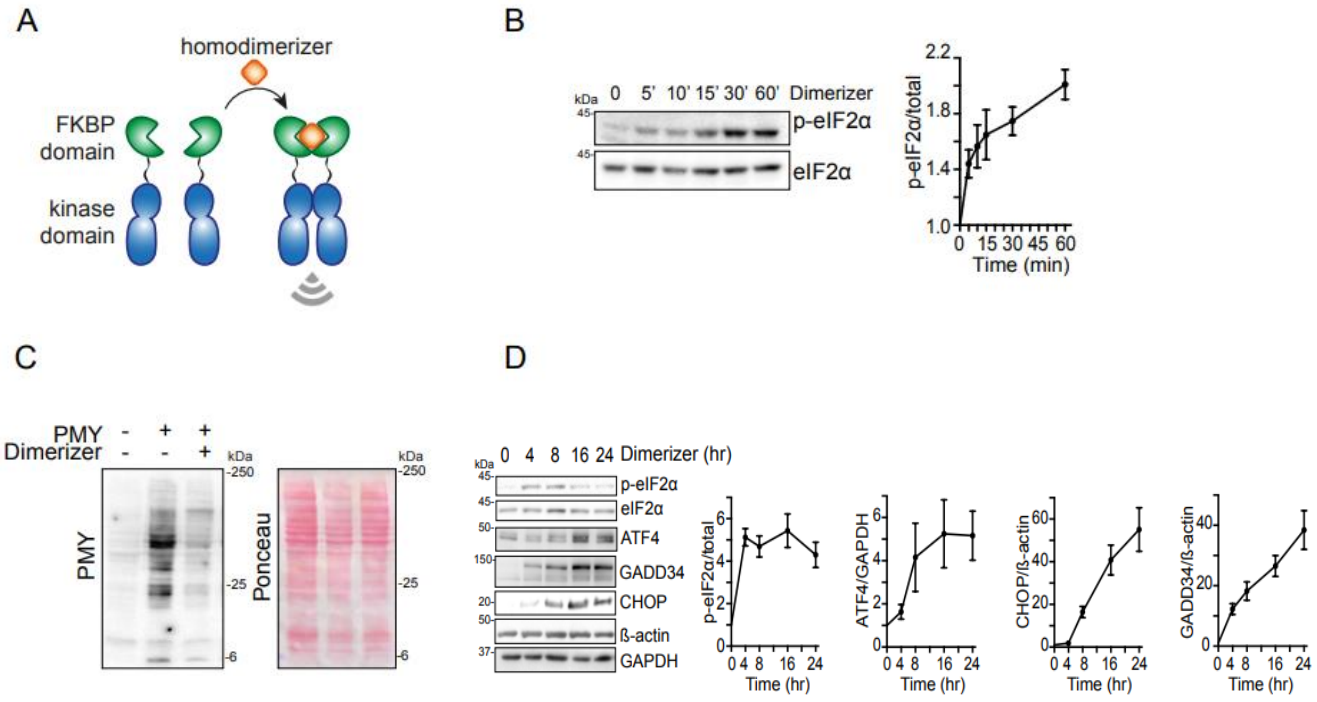

Figure 5. FKBP-PKR activates the canonical ISR signaling pathway. (A) Schematic representation of the pharmacogenetic approach for PKR activation using a synthetic dimerizer ligand. (B) Western blots showing forced-dimerization of PKR results in phosphorylation of eIF2α. Right panel: quantification of the extent of eIF2α phosphorylation (mean and SEM, N = 3). (C) Western blot showing forced-dimerization of PKR results in global protein synthesis shutdown as assessed by abundance of puromycilated peptides. (D) Western blots showing forced-dimerization of PKR results in induction of canonical ISR target genes. ß-actin, GAPDH: loading controls. The right panels show the quantification of the data (mean and SEM, N = 3).

Figure S5. Generation of a stable cell line expressing FKBP-PKR. (A) Schematic representation of FLAG-tagged FKBP-PKR construct. The CMV promoter regulates FKBP-PKR and GFP expression. (B) Western blot showing endogenous PKR depletion using CRISPRi. GAPDH, loading control.

A common ISR driven cell-fate control mechanism

1. Stress-free activation of the ISR induces DR5 and apoptosis

Treatment of cells bearing FKBP-PKR with the homodimerizer led to a greater than 4-fold induction of the DR5 mRNA, with levels that peaked at 8 hours after adding the small molecule ligand (Fig. 6A). The rise in DR5 mRNA levels was mirrored by a time-dependent accumulation of DR5 (approximate 2-fold induction at 16 hours for DR5L) protein after the addition of the homodimerizer (Figs. 6B, C). Expectedly, these changes in DR5 were accompanied by the processing of procaspase-8 and cleavage of PARP1 upon activation of FKBP-PKR with the homodimerizer (Figs. 6D, E). Alongside our results showing overexpression of phosphomimetics eIF2α^{S51D} drives DR5 accumulation (Fig 4 F-H), these results with homodimerizer-driven FKBP-PKR activation indicate that DR5 can be induced in a stress-input agnostic manner to initiate apoptosis downstream of the ISR.

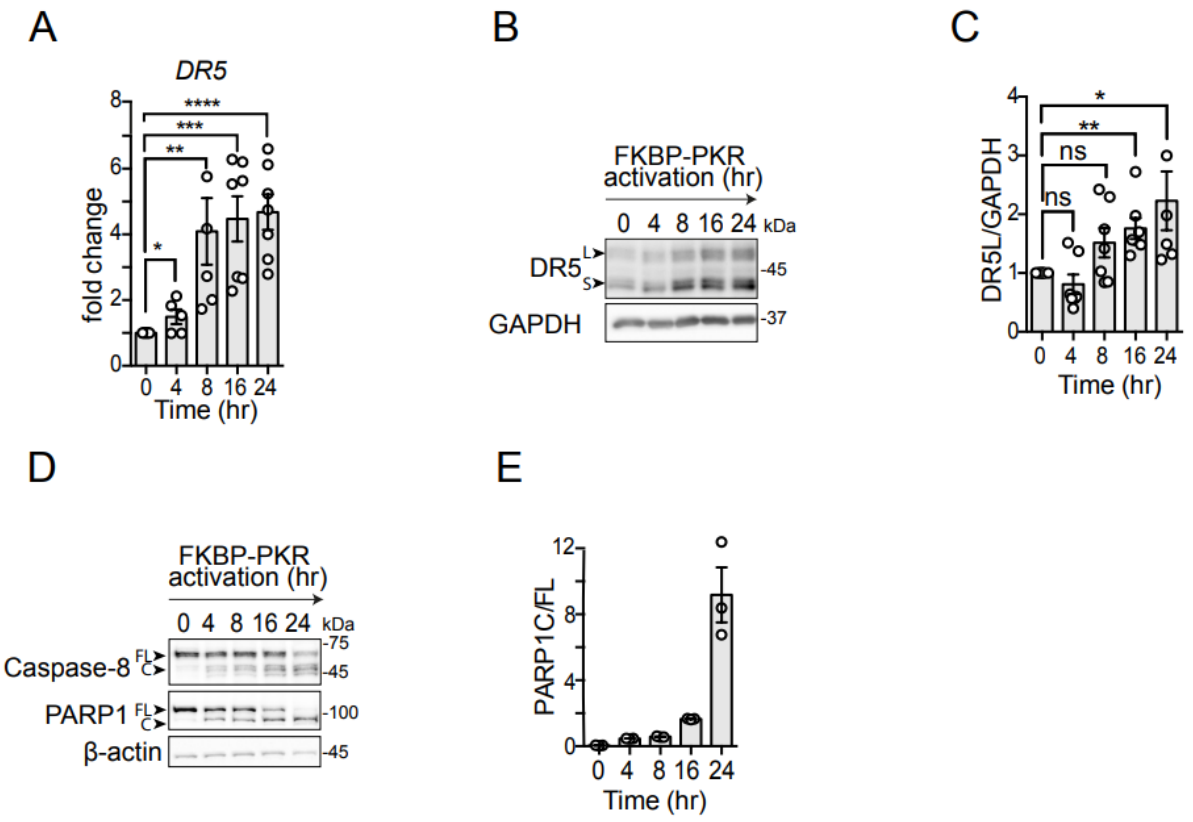

Figure 6. Stress-free activation of the ISR induces DR5 and caspase-8 cleavage. (A) qRT-PCR analysis of DR5 mRNA levels after activation of FKBP-PKR in H4 cells (mean and SEM, N = 7, ****$P < 0.0001$, ***$P < 0.001$, **$P < 0.01$, *$P < 0.05$ unpaired Student's t-test, non-parametric). (B) Western blot showing upregulation of DR5 isoforms after activation of FKBP-PKR. GAPDH: loading control. (C) Densitometry quantification of the long DR5 isoform (mean and SEM, N = 5, **$P < 0.01$, *$P < 0.05$, ns= not significant, unpaired Student's t-test, non-parametric) (D) Western blot showing caspase-8 and PARP1 cleavage after FKBP-PKR activation. GAPDH: loading control. (E) Densitometry quantification of PARP1 cleavage upon FKBP-PKR activation at the indicated time points (mean and SEM, N=3).

2. Apoptosis downstream of the ISR requires DR5

To test the dependence of the ISR cell death program on DR5, we knocked down DR5 using CRISPRi in H4 cells in cells bearing FKBP-PKR (Fig. S7A) and monitored the induction of apoptosis upon treatment with the homodimerizer. CRISPRi-mediated depletion of DR5 resulted in a significant reduction in the activation of caspase-8 and caspase-3 (Fig. 7A), substantiating the notion that DR5 is a primary determinant of ISR-induced apoptosis.

Apoptosis is controlled by extrinsic (death receptor-dependent) and intrinsic (mitochondria-dependent) interconnected signaling pathways that converge on the activation of executioner caspases. The pro-apoptotic protein BID, cleaved by caspase-8, bridges the extrinsic and intrinsic pathways (Fulda & Debatin, 2006). The active, truncated form of BID, tBID, promotes mitochondrial membrane permeabilization and cytochrome c release, triggering apoptosome formation and caspase-9 activation (Korsmeyer et al, 2000). Thus, we reasoned that a stress-free ISR induced by activation of FKBP-PKR enlists the intrinsic apoptosis pathway downstream of caspase-8. To test whether the ISR engages intrinsic apoptosis signals, we stably overexpressed the pro-survival protein BCL-XL, which inhibits mitochondrial membrane permeabilization (Billen et al, 2008) in cells bearing FKBP-PKR treated with the small molecule ligand. These experiments indicated that forced expression of BCL-XL forestalled cell death elicited by activation of FKBP-PKR as measured by PI staining (Fig. 7B). Expectedly, and attesting to ISR involvement, treatment of cells in which we activated FKBP-PKR with ISRIB restored cell viability almost completely, as did treatment with the pan-caspase inhibitor Z-VAD-FMK

(approximately 28% cell death down to 12% Fig. 7C compare columns 1 to columns 3 and 4, respectively), corroborating ISR and caspase involvement (Fig. 7C). Notably, the genetic depletion of DR5 fully restored cell viability in cells in which we activated FKBP-PKR to levels that mirrored those of the untreated controls (approximately 28% cell death down to 8% Fig. 7C compare columns 1 and 6), indicating that the “pure-ISR” driven cell-death is solely DR5 dependent. Moreover, the depletion of DR5 alone had no effects on cell viability (Fig. 7C compare columns 1 and 5), and knockdown of DR5 strongly restored cell viability in H4 cells treated with pharmacological ISR inducers (Figs. 7D, S7C), further substantiating the notion that DR5 is required to induce apoptosis in the terminal ISR.

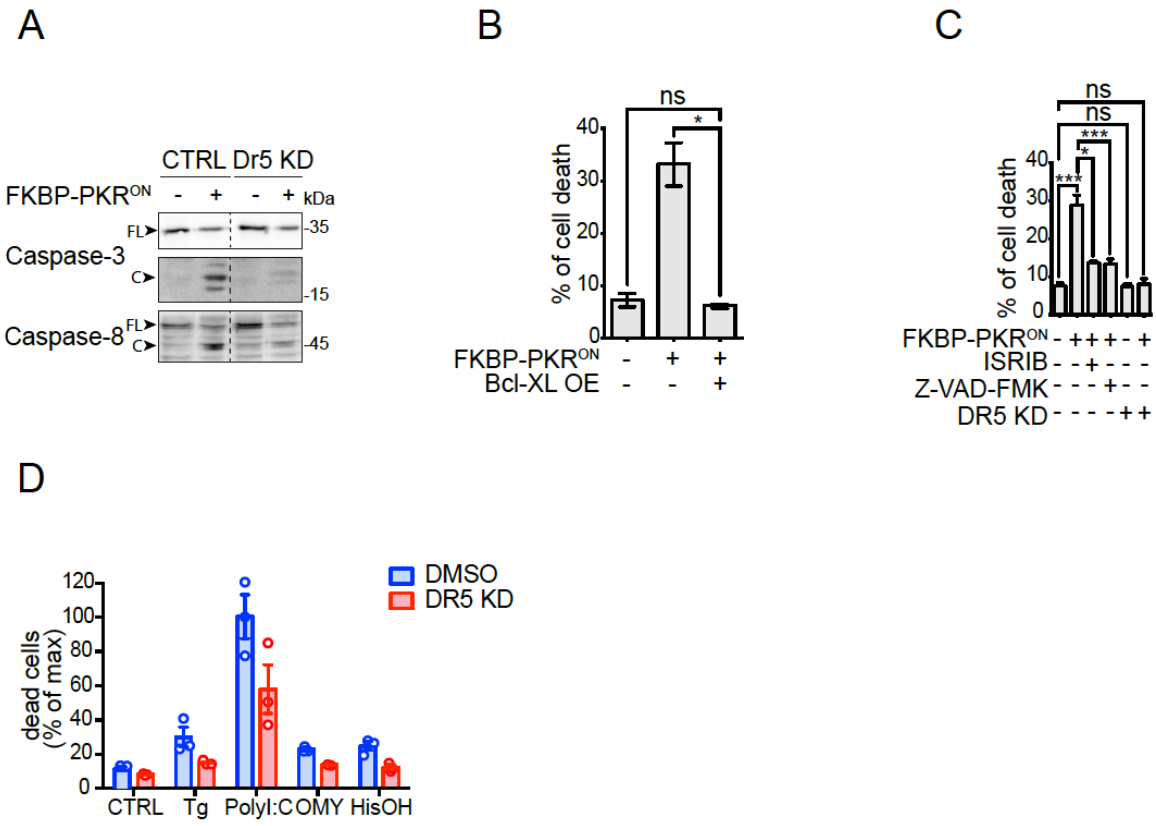

Figure 7. Cell-autonomous apoptosis downstream of the ISR requires DR5 and caspase activity. (A) Western blot showing a lack of caspase-8 and caspase-3 activation upon DR5 knockdown in H4 cells in which we activated FKBP-PKR. (B) Flow cytometry quantification of cell death after propidium iodide staining of H4 cells in which we activated FKBP-PKR and overexpressing BCL-XL (mean and SEM, N = 3, *P < 0.05, unpaired Student's t-test, non-parametric). (C) Flow cytometry quantification of cell death after propidium iodide staining in H4 cells treated with the ISR inhibitor ISRIB, the pan-caspase inhibitor Z-VAD-FMK, and upon genetic depletion of DR5 by CRISPRi (mean and SEM, N = 3, ***P < 0.001, *P < 0.05, ns= not significant, unpaired Student's t-test, non-parametric). (D) Flow cytometry quantification of cell death after propidium iodide staining in H4 DR5 CRISPRi cells treated with ISR pharmacological activators (mean and SEM, N = 3, ****P < 0.0001 One-way ANOVA).

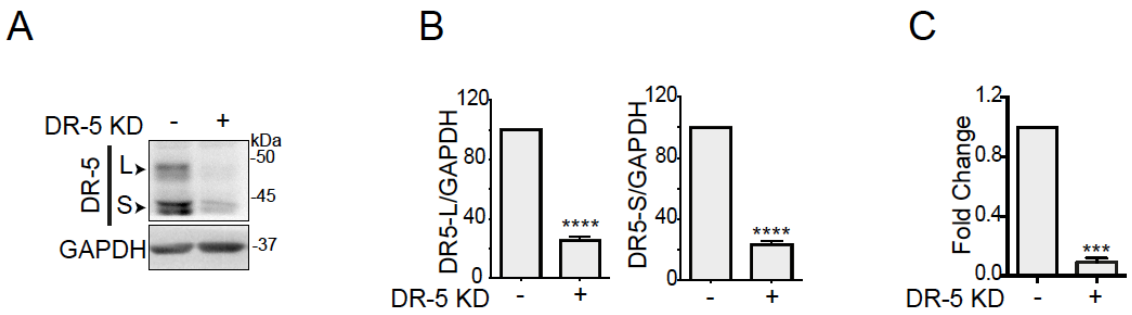

Figure S7. Generation of DR5-deficient cell lines (A) Western blot showing the extent of CRISPRi-mediated knock-down of DR5 in H4 FKBP-PKR cells. GAPDH; loading control. (B) Densitometry quantification of the DR5 short and long isoforms upon genetic depletion by CRISPRi (mean and SEM, N = 3, ****$P < 0.0001$, unpaired Student's t-test, non-parametric). (C) Quantitative real-time PCR analysis showing the levels of DR5 in H4 cells (mean and SEM, N = 3, ***$P < 0.001$, unpaired Student's t-test, non-parametric).

3. Activation of DR5 downstream of the ISR is intracellular and ligand-independent

It is known that tumor necrosis factor (TNF)-related apoptosis inducing ligand (TRAIL) binds DR5 in the plasma membrane inducing its assembling into higher-order oligomers and the subsequent apoptotic cascade. However, it was previously shown that during persistent ER stress—which activates the PERK branch of the ISR—DR5 activates intracellularly in a ligand-independent fashion (Lu et al, 2014; Lam et al, 2020). Based on this observation, we wondered whether DR5 accumulates intracellularly and signals similarly, independent of its ligand TRAIL, upon induction of a stress-free ISR. To answer this question, we first measured the levels of TRAIL mRNA by qRT-PCR and found that TRAIL mRNA levels rise in cells bearing FKBP-PKR in response to treatment with the -homodimerizer. Still, its upregulation subsides in a time-dependent manner (Fig. 8A, note that the qRT-PCR cycle threshold value (Ct) first decreases at 4 hours after FKBP-PKR activation and increases as time advances, indicating a rise and decay of the TRAIL mRNA levels). These results suggest that TRAIL might be secreted from cells in which we activate the ISR, albeit at modest levels.

Next, we investigated whether any secreted TRAIL could engage DR5 at the plasma membrane to signal apoptosis in an autocrine or paracrine fashion. To this end, we exposed cells in which we activated FKBP-PKR with the homodimerizer to a DR5-neutralizing Fc antibody fragment (FcDR5). Treatment with FcDR5 did not prevent the activation of caspases-3 and -8, or cleavage of PARP1 (Figs. 8B, C), nor did it block cell death (Fig. 8D) in response to FKBP-PKR activation, indicating that

plasma membrane DR5 is not required for transducing death signals upon activation of a terminal ISR.

Finally, we examined the subcellular localization of DR5 upon induction of a stress-free ISR by activation of FKBP-PKR. Treatment of cells bearing FKBP-PKR with the homodimerizer led to an accumulation of DR5 in the *cis*-Golgi apparatus, as evidenced by co-staining with the *cis*-Golgi apparatus marker GM130 in immunofluorescence analyses (Fig. 8E). Strikingly, the intracellular localization of DR5 to the *cis*-Golgi apparatus elicited by a stress-free activation of the ISR was indistinguishable from that produced by ER stress-inducing agents (Fig. 8E) and (Lu et al, 2014; Lam et al, 2020), indicating that intracellular retention of DR5 in the *cis*-Golgi apparatus is a common feature of the terminal ISR. Together, these results substantiate that the terminal ISR engages a common, unconventional, cell-autonomous apoptosis mechanism that relies on intracellular DR5 activation.

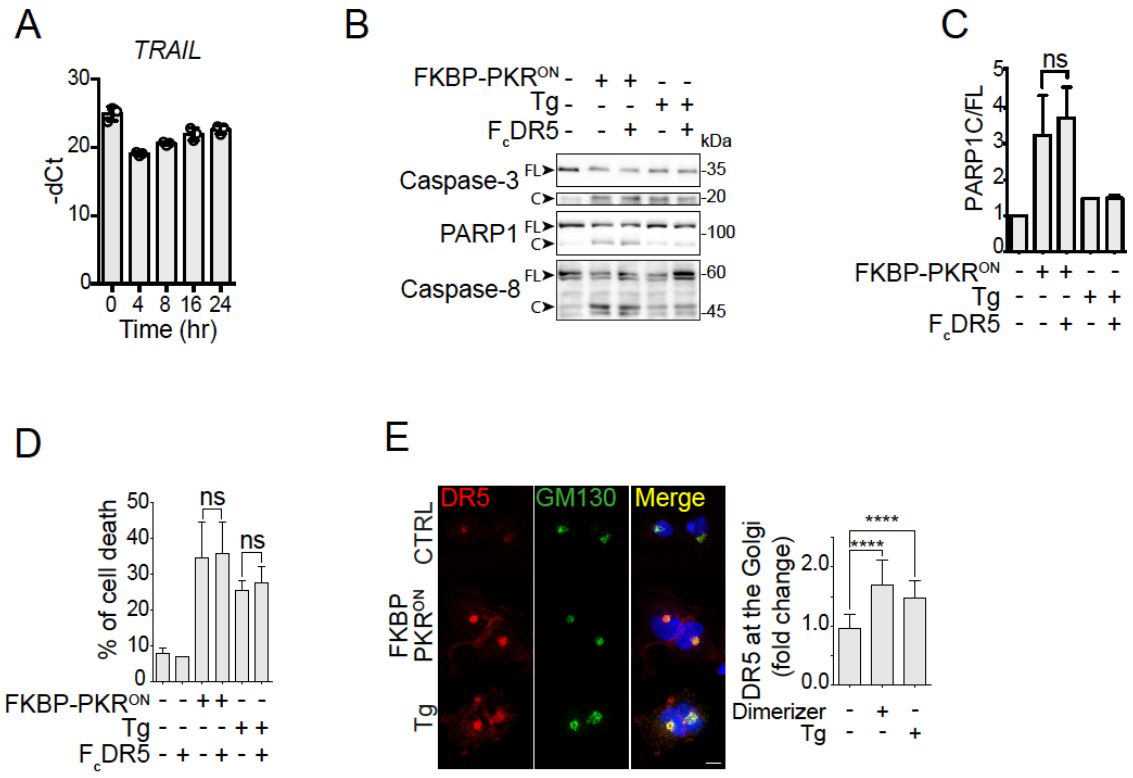

Figure 8. Stress-free activation of the ISR leads to intracellular ligand-independent activation of DR5. (A) Quantitative real-time PCR analysis showing the levels of TRAIL mRNA after activation of FKBP-PKR. (B) Western blot showing that blocking plasma membrane DR5 with FcDR5 does not impede the activation of caspase-3, caspase-8 and PARP1 cleavage in H4 cells in which we activated FKBP-PKR. (C) Densitometry quantification of PARP1 cleavage upon activation of FKBP-PKR and co-treatment with FcDR5 (mean and SEM, N = 3, ns = not significant, unpaired Student's t-test, non-parametric). (D) Flow cytometry quantification of cell death after propidium iodide staining of H4 cells treated with FcDR5 or thapsigargin (Tg, positive control). (E) Representative immunofluorescence images showing that DR5 co-localizes with the *cis*-Golgi apparatus marker GM130 upon induction of the ISR with natural stress inputs or in stress-free conditions after. activation of FKBP-PKR. Right panel: quantification of extent of localization of DR5 in the *cis*-Golgi apparatus in immunofluorescence analyses. (mean and SEM, N = 3, n>1000, ****$P < 0.001$, *$P < 0.05$, unpaired Student's t-test, non-parametric).

DISCUSSION

The ISR and the UPR share a common mechanism for cell fate control

Using orthogonal approaches, in this chapter, our findings demonstrate that the terminal ISR initiates a cell-autonomous apoptosis mechanism that relies on intracellular activation of DR5 and engagement of the extrinsic and intrinsic apoptosis pathways. Activation of this cell-autonomous apoptosis mechanism depends solely on eIF2α phosphorylation, and therefore is common to all branches of the ISR, including by synthetically engineered activation of sensors. We base this conclusion on multiple lines of evidence. First, natural, lethal ISR stress inputs upregulate DR5 mRNA and protein (Figs. 4A, B), and actuate apoptosis downstream of DR5 (Fig. 4B), as does the stress-free activation of the ISR using a synthetic biology tool (Figs. 6A-E). Second, the ISR inhibitor ISRIB reverses the upregulation of DR5 and subsequent cell death triggered by the ISR (Figs. 4C, 3C), indicating that cell death signals pass through phosphorylation of eIF2α. Third, cells lacking DR5 are less susceptible to cell death triggered by classical ISR inducers (Fig. 7D) as well as by a stress-free ISR (Fig. 7C). Fourth, DR5 accumulates in the *cis*-Golgi apparatus in response to classical ISR inducers and upon stress-free induction of the ISR (Fig. 8E) and blocking plasma-membrane DR5 with a neutralizing antibody had no effect on cell viability (Figs. 8B, 8C), indicating intracellular DR5 activation during the terminal ISR.

For continued organismal health, the ISR must accurately interpret information about stress states and actuate accordingly to control homeostatic or terminal outputs. On the one hand, tailored homeostatic outcomes are likely executed through ISR kinase signal codes, which could result from additional ISR kinase substrates and

interactors and from accessibility to different pools of eIF2α. On the other hand, considering all ISR sensor kinases pass signals through a core relay, eIF2α, the terminal ISR is likely to employ an off-the-shelf mechanism downstream of eIF2α that funnels information about an irreparable critical state to a common executor, DR5. Our data support this notion, indicating that the terminal ISR operates through a pro-apoptotic relay consisting of phospho-eIF2α→CHOP→DR5 (Yamaguchi & Wang, 2004; Lu et al, 2014; Castelli et al, 1998; Besch et al, 2009; Siddiqui et al, 2015).

It is noteworthy that during ER stress, intracellular DR5 has been postulated to be activated by unfolded protein ligands (Lam et al, 2020). While we cannot formally exclude the possibility that our synthetic ISR activation approach induces some mild accumulation of unfolded proteins that can serve as DR5 activating ligands, it is unlikely it does so to a level that is comparable to that elicited by classic ER poisons (e.g., thapsigargin or the N-linked glycosylation inhibitor tunicamycin) or forced-expression of a single ER folding-mutant protein, such as myelin protein zero (Lam et al, 2020). Nevertheless, considering that some misfolded proteins bind DR5, it remains plausible that a sustained ISR may induce the accumulation of a single or a subset of select ER client protein(s) that may engage DR5 leading to its activation. Future -omics studies (coupled RNAseq and proteomics) in cells in which we activate the ISR synthetically may shed light on the mechanism of activation of DR5 during the terminal ISR. It is intriguing that the terminal ISR engages a cell surface death receptor unconventionally. Because plasma membrane DR5 is not required for the terminal ISR, and the bulk of the protein is confined to the secretory apparatus, additional

mechanisms may hold DR5 inside the cell. This is an intriguing possibility that remains to be investigated.

Our results also indicate a potential node for therapeutic intervention in the ISR. A dysregulated ISR has been observed in numerous neurocognitive disorders (Bando et al, 2005; Zhu et al, 2019; Bond et al, 2020; Krukowski et al, 2020; Halliday et al, 2015). Therefore, a terminal ISR may lead to neural cell loss. Antisense oligonucleotides, which have shown efficacy in neurodegenerative diseases including Duchenne's muscular dystrophy, spinal muscular atrophy, and hereditary transthyretin-mediated amyloidosis (Nguyen & Yokota, 2019; Relizani & Goyenvalle, 2018; Chen, 2019; Wood et al, 2017; Gales, 2019), could be deployed to target DR5 and prevent neural cell loss. Regardless of potential therapeutic applications, identifying a common mechanism controlling cell death during prolonged ISR signaling advances our understanding of how the ISR operates to maintain the health of tissues: customized homeostatic solutions or a one-size-fits-all terminal response.

CHAPTER 3

Cross-connectivity between the ISR and the UPR revealed through a chemical genetics approach

To investigate the gene expression program selectively activated by stress-free ISR, we took an unbiased approach and performed RNA sequencing (RNA-seq) in cells in which we activated the ISR by ligand-induced dimerization of the synthetic sensor. In this chapter, we show that, surprisingly, ISR signaling activates the ER stress sensor IRE1 in the absence of ER stress. While it is well established that the PERK branch of the UPR initiates the ISR, this finding suggests a novel mechanism of ISR activation of a specific branch of the UPR, possibly to buffer DR5 activation and the initiation of cell death pathways.

Synthetic activation of a pure ISR regulates the UPR

To learn more about the gene expression program selectively induced by a stress-free ISR, we collected time-resolved gene expression profiles by RNA-seq in cells in which we activated FKBP-PKR for 4, 12 and 18 hrs (Fig. 9). As expected, FKBP-PKR activation induced gene expression programs that are associated with the ISR, such as apoptosis and inflammation (Tian et al, 2021; Reverendo et al 2019; Kang & Tang, 2012) which are the outcome of sustained ISR signaling during continuous stress (Fig.9).

To our surprise, we also found a time-dependent enrichment of UPR gene expression signatures after FKBP-PKR activation (Fig.9), indicating that sustained FKBP-PKR activity induces the UPR.

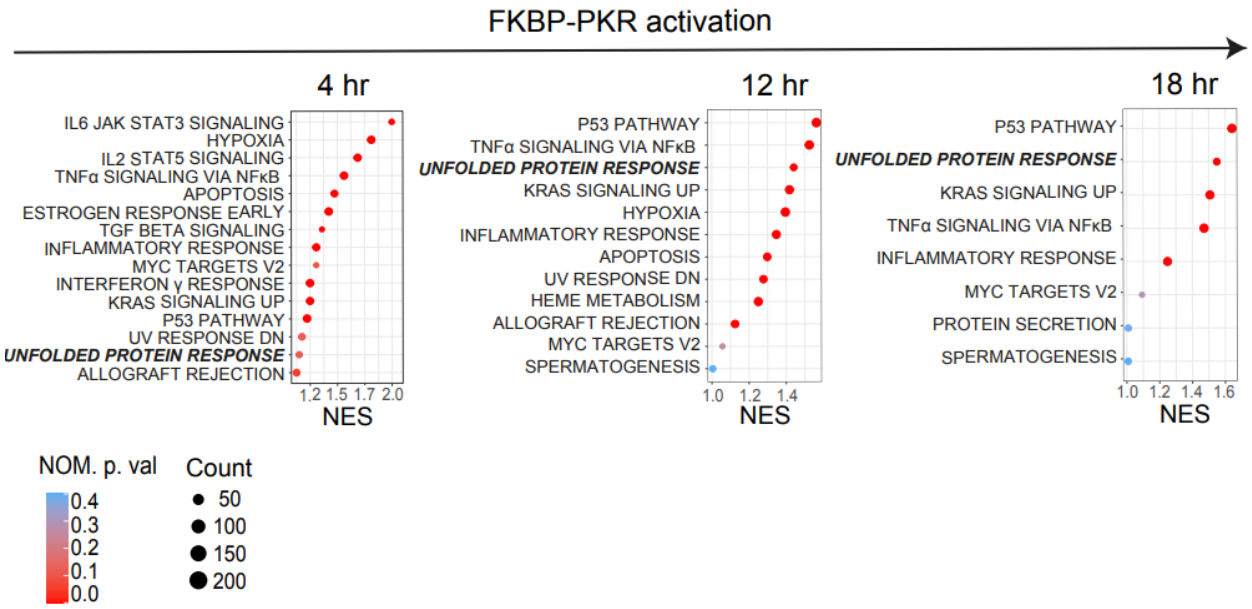

Figure 9. KEGG pathway enrichment analysis of cells in which we activated FKBP-PKR. Pathway enrichment of differentially expressed genes in cells in which FKBP-PKR was activated for 4, 12 and 18 hours. The X-axis indicates the normalized enrichment score (NES) for each of the pathway. The bubble size indicates the number of genes. The color bar indicates the normalized p-value. Data obtained from three biological replicates.

The ISR selectively activates IRE1

Since the activation of FKBP-PKR induced a UPR gene signature, we next decided to examine the involvement of each UPR sensor upon stress-free ISR induction. Besides the expected common ISR/UPR gene expression signature (e.g., those gene expression programs controlled by ATF4 and CHOP), we also found that known genes that are regulated by the IRE1 and ATF6 were upregulated, such as XBP1, DNAJB9 and BiP (Fig. 10A). Moreover, we found that the levels of manually curated IRE1 RIDD targets (obtained from our previous RNA-Seq datasets; Acosta-Alvear et al, 2018) decreased in response to FKBP-PKR activation, suggesting a direct engagement of IRE1 (Fig.10B).

Consistent with the RNA-seq data, we found that in response to homodimerizer induced activation of FKBP-PKR, IRE1 phosphorylation levels increase starting at 4 hours and the consequent robust splicing of the XBP1 mRNA is observed by 16 hours (Figs. 10C, F). In line with these results, XBP1s target genes BiP and DNAJB9 were also upregulated (Figs. 10G, H), and known IRE1 RIDD target mRNAs encoding BLOCSC1, SCARA3, and Col6A1 were downregulated (Fig. 10I). Co-treatment with the IRE1 RNase inhibitor 4μ8C suppressed the RIDD of these mRNAs (Fig.10I), confirming that FKBP-PKR activates IRE1.

As mentioned in the previous chapter, the DR5 mRNA is a RIDD target (Lu et al, 2014). Thus, we next tested whether activation of FKBP-PKR leads to DR5 mRNA RIDD. As observed previously, homodimerizer-induced oligomerization of FKBP-PKR induces DR5 mRNA. In the presence of 4μ8C, we found a further, modest increase in

DR5 mRNA levels in cells in which we activated FKBP-PKR (Fig.10J), suggesting a modest contribution of RIDD in the conditions tested.

Previous findings suggest that IRE1 and PERK use a similar mechanism to sense ER stress through their respective, and functionally interchangeable, lumenal sensor domains (Adams et al, 2019; Bertolotti et al, 2000). Therefore, we reasoned that if FKBP-PKR activates IRE1, it could also activate PERK. In contrast to Tg treatment, FKBP-PKR activation for 72 hrs did not trigger PERK activation analyzed by Western blot (Fig.10K), suggesting that if PERK is active in these conditions, its levels are below the limit of immunodetection.

Next, we sought to investigate whether ATF6 is activated by FKBP-PKR. Since BiP, an ER lumenal chaperone, is regulated by both XBP1 and ATF6 during ER stress (Yamamoto et al, 2016; Hirota et al, 2006; Hillary and FitzGerald, 2018), we used BiP mRNA upregulation as a proxy to analyze the ATF6 activation. FKBP-PKR activation led to BiP mRNA upregulation (Fig. 10L), consistent with the possible involvement of ATF6. To test if the upregulation of BiP upon activation of FKBP-PKR resulted from ATF6 activity, we compared the BiP expression levels in cells in which we activated FKBP-PKR treated with ATF6 inhibitor ceapin (Gallagher & Walter, 2016). We found that ceapin did not block BiP mRNA upregulation (Fig. 10L), although it did reduce BiP mRNA accumulation triggered by the ER stress inducer tunicamycin (Fig. 10L). Furthermore, genetic depletion of ATF6 by CRISPRi in cells in which we activated FKBP-PKR had no effect on BiP mRNA induction and upregulation (Fig.10L). In line with these observations, our RNA-seq data set did not show significant changes in gene expression levels of known ATF6 targets (Fig.10M), including the well-known

ATF6 canonical target, GRP94/HSP90B1 (Fig. 10N). Taken together, these findings suggest that a stress-free ISR selectively activates the IRE1 branch of the UPR.

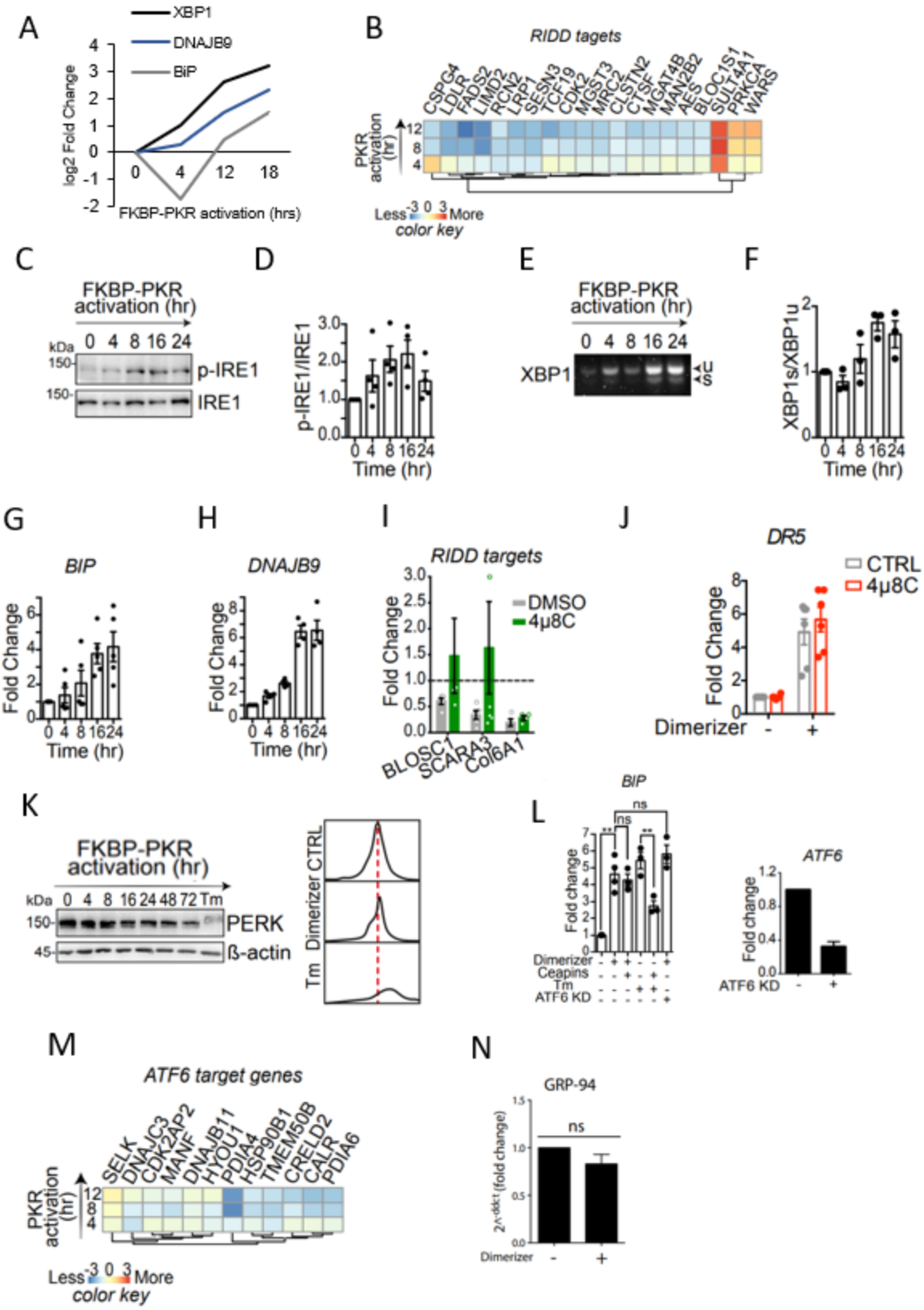
A
XBP1
DNAJB9
BiP
log2 Fold Change
FKBP-PKR activation (hrs)
B
RIDD tagets
CSPG4 LDLR FADS2 LIMD2 RCN2 LRP1 SESN3 TCF19 CDK2 MGST3 MRC2 CLSTN2 CTSF MGAT4B MAN2B2 AES BLOC1S1 SULT4A1 PRKCA WARS
PKR activation (hr)
Less -3 0 3 More
color key
C
FKBP-PKR activation (hr)
kDa 0 4 8 16 24
p-IRE1
IRE1
D
p-IRE1/IRE1
Time (hr)
E
FKBP-PKR activation (hr)
XBP1
F
XBP1s/XBP1u
Time (hr)
G
BIP
Fold Change
Time (hr)
H
DNAJB9
Fold Change
Time (hr)
I
RIDD targets
DMSO
4μ8C
Fold Change
BLOSC1 SCARA3 Col6A1
J
DR5
CTRL
4μ8C
Fold Change
Dimerizer
K
FKBP-PKR activation (hr)
kDa 0 4 8 16 24 48 72 Tm
PERK
ß-actin
Dimerizer CTRL
Tm
L
BIP
Fold change
Dimerizer
Ceapins
Tm
ATF6 KD
ATF6
Fold change
ATF6 KD
M
ATF6 target genes
SELK DNAJC3 CDK2AP2 MANF DNAJB11 HYOU1 PDIA4 HSP90B1 TMEM50B CRELD2 CALR PDIA6
PKR activation (hr)
Less -3 0 3 More
color key
N
GRP-94
ns
Dimerizer

Figure 10. Stress-free ISR activates IRE1 but no ATF6 and PERK. (A) Expression levels of select genes obtained from RNA-seq data in cells in which we activated FKBP-PKR. (B) Heatmap of RNA-seq expression data showing the RIDD target genes. (C) Western blot showing upregulation of p-IRE1 in H4-FKBP-PKR cells. (D) Densitometry quantification of the Western blot data for p-IRE1 (N=4). (E) Semi-quantitative PCR using primers that amplify both XBP1u and XBP1s from cDNA, separated on 3% agarose. (F) Densitometry quantification of the semi-quantitative PCR data for XBP1u and XBP1 (N=3). (G-H) qRT-PCR analysis of BiP and DNAJB9 mRNA levels in FKBP-PKR cells treated with homodimerizer for the indicated time (mean and SEM, N = 5). (I) qRT-PCR analysis of RIDD targets BLOSC1, SCARA3 and Col6A1 mRNA levels in FKBP-PKR cells treated with homodimerizer. The graph shows the IRE1 RNase inhibitor 4μ8C recovers the levels of these mRNAs (mean and SEM, N = 5). (J) qRT-PCR analysis of DR5 mRNA levels in FKBP-PKR cells treated with homodimerizer in the presence of 4μ8C (mean and SEM, N = 6). (K) Western blot showing no activation of PERK after activation of FKBP-PKR. GAPDH: actin. (L) Left: qRT-PCR analysis of BiP mRNA levels in wild-type or ATF6-KD FKBP-PKR cells treated with homodimerizer, ceapins and/or Tm. Right: qRT-PCR analysis showing the levels of ATF6 in FKBP-PKR cells. (M) Heatmap of subset of selected ATF6 target genes. (N) qRT-PCR analysis showing the levels of ATF6 target GRP-94 in FKBP-PKR cells.

Selective activation of IRE1 by the ISR requires eIF2α phosphorylation

Because the four ISR kinases converge on eIF2α, we reasoned that IRE1 activation by the ISR could require eIF2 phosphorylation. To test this hypothesis, we co-treated cells with the homodimerizer and ISRIB, and monitored IRE1 activity. ISRIB treatment significantly reduced XBP1 mRNA splicing following FKBP-PKR activation (Fig. 11A), it blocked the upregulation of the XBP1s target genes DNAJB9 and BiP, and it restored the levels of BLOSC1S1 (Figs. 11B-D).

To discard the possibility that the aforementioned effects were amplified by PKR-specific activities, we used the H4 neuroglioma cell line overexpressing the phosphomimetic eIF2α^{S51D} mutant described in chapter 2. In these conditions, we still observed IRE1 phosphorylation, which was accompanied by induction of XBP1 mRNA splicing, the upregulation of XBP1s targets BiP and DNAJB9, and reduction in the mRNA levels of BLOS1, SCARA3, and Col6A1 (Figs. 11E-J).

In a parallel approach, we treated human embryo kidney (HEK293) cells with oligomycin to activate HRI and induce the ISR (Guo et al, 2020). In line with our previous observations, oligomycin treatment induced XBP1 mRNA splicing, which was abrogated by co-treatment with ISRIB or 4μ8C (Fig.11K). Taken together, these results indicate that IRE1 activation is part of a common ISR signaling relay downstream of eIF2α phosphorylation.

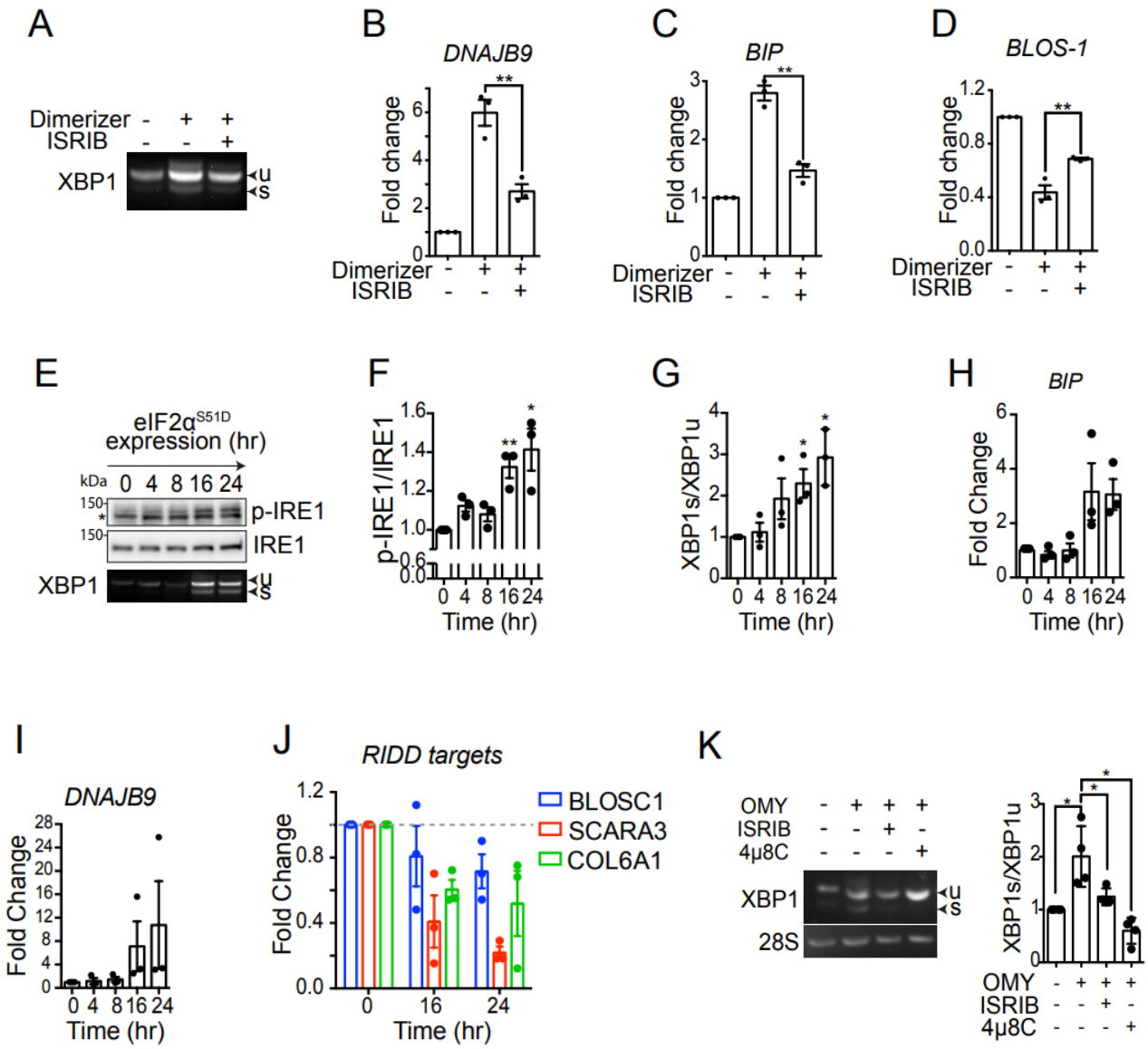

Figure 11. IRE1 activation is downstream eIF2α phosphorylation. (A) Semi-quantitative PCR using primers that amplify both XBP1u and XBP1s from cDNA extracted from FKBP-PKR cells treated with the ISR inhibitor ISRIB, separated on 3% agarose. (B-D) qRT-PCR analysis of DNAJB9, BiP and BLOSC1 mRNA levels in activated FKBP-PKR cells treated with ISRIB (mean and SEM, N = 3). (E) Top: Western blot showing upregulation of p-IRE1 in H4 cells expressing FLAG epitope-tagged eIF2α^{S51D} and treated with doxycycline for the indicated time. Bottom: Semi-quantitative PCR using primers that amplify both XBP1u and XBP1s, separated on 3% agarose. (F) Densitometry quantification of the Western blot data for p-IRE1 (N=3).

(G) Densitometry quantification of the semi-quantitative PCR data for XBP1u and XBP1 (N=3). (H-I) qRT-PCR analysis of BiP and DNAJB9 mRNA levels in in H4 cells expressing FLAG epitope-tagged eIF2α^{S51D} cells treated with doxycycline for the indicated time (mean and SEM, N = 3). (J) qRT-PCR analysis of RIDD targets BLOSC1, SCARA3 and Col6A1 mRNA levels in H4 cells expressing FLAG epitope-tagged eIF2α^{S51D} treated with doxycycline (mean and SEM, N = 3). (K) Left panel: Semi-quantitative PCR using primers that amplify both XBP1u and XBP1s from cDNA extracted from HEK293 cells treated with the oligomycin, ISRIB and/or 4μ8C, separated on 3% agarose. Right panel: Densitometry quantification of the semi-quantitative PCR data for XBP1u and XBP1 (N=4).

The ISR activates IRE1 independently of protein folding- or lipid bilayer-stress

Besides detecting protein folding perturbation in the ER lumen, IRE1 is also able to sense lipid bilayer-stress in the ER membrane. While the lumenal domain is in charge of sensing the unfolded proteins (Gardner & Walter, 2011; Karagöz et al, 2017), lipid bilayer-stress requires IRE1's transmembrane amphipathic helical domain (Halbleib et. al, 2017). Since our approach to induce a stress-free ISR does not activate the canonical UPR (Fig. 10), we hypothesized that the selective activation of IRE1 could be triggered by selective unfolded proteins or lipid-stress inputs. On one hand, to test whether ISR-driven IRE1 activation is driven by unfolded proteins, we generated an IRE1 mutant lacking its N-terminal ER lumenal domain (IRE1ΔLD) expressed under the control of a tetracycline-inducible promoter. We then introduced IRE1ΔLD into U2OS-IRE1 knockout cells expressing FKBP-PKR and analyzed IRE1ΔLD's signaling ability. Surprisingly, activation of FKBP-PKR triggered IRE1ΔLD activation and downstream signaling, as evidenced by induction of XBP1 mRNA splicing and the downregulation of RIDD targets (Fig. 12A). On the other hand, to test whether stress-free ISR-driven IRE1 activation is triggered by lipid bilayer stress, we introduced a point mutation in the transmembrane domain of the IRE1ΔLD (IRE1ΔLD^{W457A}) that blunts IRE1 sensitivity to lipid saturation (Halbleib et al, 2017; Ho et al, 2020). Remarkably, IRE1ΔLD^{W457A}, which is double-deficient in its stress sensing capabilities, was still able to activate canonical IRE1 downstream signals, including XBP1 mRNA splicing and RIDD (Fig. 12B).

Next, we sought to investigate whether IRE1ΔLD^{W457A} is able to signal upon thapsigargin treatment. Expectedly, activation of the UPR triggered IRE1ΔLD^{W457A}

activation, as evidenced by the IRE1 phosphorylation and downstream induction of XBP1 splicing (Fig. 12C), indicating that PERK, upon Tg treatment, activates the ISR, followed by the phosphorylation of eIF2α and subsequent activation of IRE1. Together, these results indicate that neither IRE1's ER lumenal domain nor its lipid sensor transmembrane domain are required for transducing IRE1 signals upon ISR induction, suggesting that IRE1 activation might be driven by the cytosolic domains.

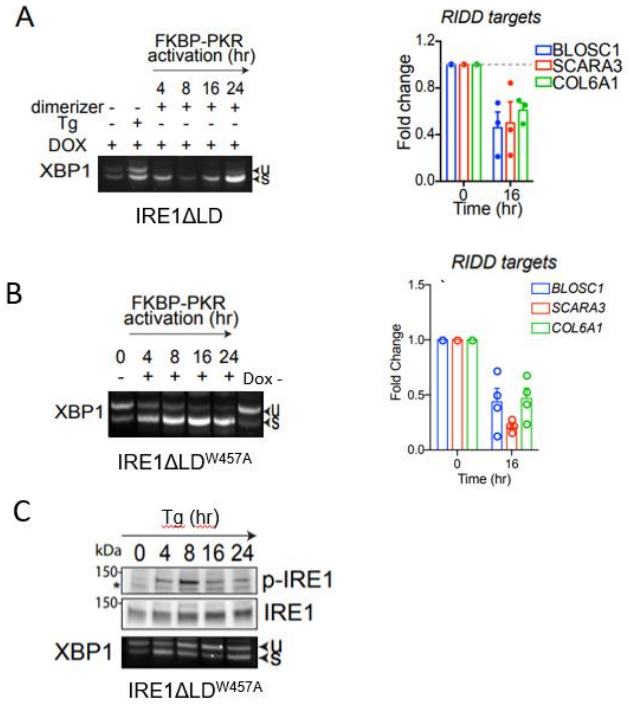

Figure 12. Protein folding- or lipid bilayer-stress do not cause ISR-dependent IRE1 activation. (A) Left panel: Semi-quantitative PCR using primers that amplify both XBP1u and XBP1s from cDNA extracted from U2OS-IRE1 knockout cells expressing IRE1ΔLD and FKBP-PKR treated with doxycycline and homodimerizer, or thapsigargin (Tg, positive control), separated on 3% agarose. Right panel: qRT-PCR analysis of RIDD targets BLOSC1, SCARA3 and Col6A1 mRNA levels in U2OS-IRE1 knockout cells expressing IRE1ΔLD and FKBP-PKR treated with doxycycline and homodimerizer (mean and SEM, N = 3). (B) Left panel: Semi-quantitative PCR using primers that amplify both XBP1u and XBP1s from cDNA extracted from U2OS-IRE1 knockout cells expressing IRE1ΔLD^{W457A} and FKBP-PKR treated with doxycycline and homodimerizer, separated on 3% agarose. Right panel: qRT-PCR analysis of RIDD targets BLOSC1, SCARA3 and Col6A1 mRNA levels in U2OS-IRE1 knockout cells expressing IRE1ΔLD^{W457A} and FKBP-PKR treated with doxycycline and homodimerizer (mean and SEM, N = 3). (C) Top: Western blot showing upregulation of p-IRE1 in U2OS-IRE1 knockout cells expressing IRE1ΔLD^{W457A} and FKBP-PKR

treated with doxycycline and homodimerizer for the indicated time. Bottom: Semi-quantitative PCR using primers that amplify both XBP1u and XBP1s, separated on 3% agarose.

ISR-driven IRE1 activation is not regulated by stress-responsive transcription factors

ISR activation first results in a repression of translation initiation due to phosphorylation of eIF2α, followed by the activation of ATF4 and CHOP transcription factors. To test if IRE1 activation depends on a factor regulated by the transcriptional re-programming of the ISR, we tested if IRE1 can be activated after knockdown of ATF4.

ATF4 is considered a main ISR transcription factor, thus we first used CRISPRi to constitutively silence ATF4 in cells expressing FKBP-PKR. This experiment yielded a near-complete abrogation of ATF4 accumulation upon ISR induction (Fig. 13A). In these conditions, we still detected IRE1 signaling as evidenced by XBP1 mRNA splicing (Fig. 13A). We next used RNAi to acutely deplete ATF4 as well as additional transcription factors that are known to be associated with the ISR, including ATF3, ATF5, and CHOP (Pakos-Zebrucka et al, 2016; Costa-Matiolli & Walter, 2020), and analyzed IRE1 signaling upon activation of FKBP-PKR. Neither the genetic depletion of ATF3, ATF4, and ATF5, alone or in combination, nor CHOP RNAi blunted the ability of FKBP-PKR to induce IRE1 signaling (Fig. 13B), suggesting that IRE1 signaling is not transcriptionally regulated by these ISR effectors.

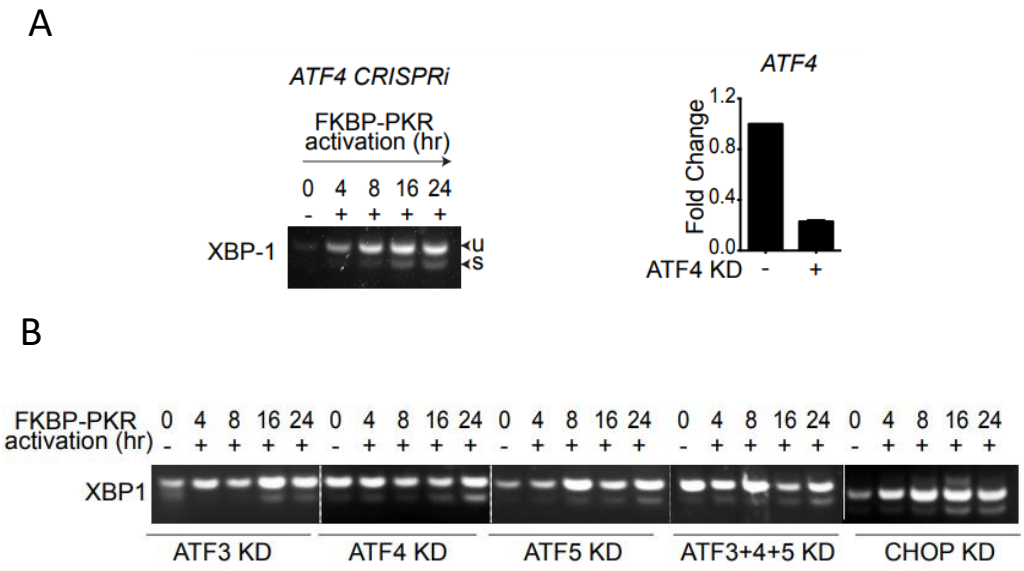

Figure 13. IRE1 is not activated by transcriptional reprogramming. (A) Left pannel: Semi-quantitative PCR using primers that amplify both XBP1u and XBP1s from cDNA extracted from H4-ATF4 knockdown cells in which we activated FKBP-PKR for the indicated times, separated on 3% agarose. Right panel: Quantitative real-time PCR analysis showing the levels of DR5 in H4 cells (mean and SEM, N = 3). (B) Semi-quantitative PCR using primers that amplify both XBP1u and XBP1s from cDNA extracted from H4-ATF3, ATF4, ATF5 and CHOP knockdown cells in which we activated FKBP-PKR for the indicated times, separated on 3% agarose.

DISCUSSION

The ISR and the UPR are interconnected

Our data identifies that the ISR activates the UPR sensor IRE1 in the absence of ER stress, establishing a novel channel of communication between these two stress responses. Thus, our findings connect the ISR and the UPR outside their shared node, the sensor kinase PERK. This conclusion is based on multiple lines of evidence. First, we examine the gene expression program selectively induced by a stress-free ISR and show an enrichment of UPR gene expression signatures overtime (Fig. 9). Second, the activation of FKBP-PKR activates IRE1 (Fig. 10C, D), which leads to the splicing of the XBP1 mRNA and upregulation of its downstream targets, and reduction in the mRNA levels of RIDD targets (Figs. 10E-I). Third, FKBP-PKR activation does not trigger the activation of the other two UPR nodes, PERK and ATF6 (Figs. 10K-N). Fourth, the ISR inhibitor ISRIB reverses the activation of IRE1, indicating that the signal passes through phosphorylation of eIF2α (Fig. 11).

ER stress induced by thapsigargin or tunicamycin typically engages all three branches of the UPR: IRE1, PERK, and ATF6. Here we find, that upon stress-free activation of ISR, IRE1 is active, while ATF6 and PERK are not active, suggesting selective activation of the IRE1 branch. Furthermore, we find that IRE1 activation does not require its lumenal domain and is not sensitive to mutations in its transmembrane domain (Fig. 12 A, B). These two domains are respectfully required for detection of unfolded proteins and lipid bilayer stress. Moreover, we observe that thapsigargin treatment in IRE1ΔLD^{W457A} cells activates the IRE1 branch (Fig 12 C), indicating the role of PERK in activating IRE1 downstream the ISR. These observations substantiate

the notion that the activation of IRE1 is a universal ISR mechanism. Together, these findings suggest that IRE1 activation by the ISR is driven from the cytosolic side. In principle, anything that stabilizes IRE1 oligomerization is capable of activating IRE1, however, the trigger in response to the ISR remains unclear.

A number of studies have identified proteins that interact with IRE1's cytosolic domain to influence UPR signaling, including posttranslational modifiers such as the ER-anchored poly-ADP-ribose-polymerase PARP16, and the tyrosine kinase ABL family member ABL-2 (Jwa &Chang, 2012; Morita et al, 2017). Indeed, FKBP-PKR activation led to an approximate 2-fold increase in the mRNA level of PARP16 and 6-fold in the mRNA level of ABL-2 in our RNA-seq. data (data not shown), suggesting their putative involvement in IRE1 activation. However, our candidate approach revealed that neither of the ISR transcription factors ATF3,4,5, nor CHOP blunted the ability of FKBP-PKR to induce IRE1 signaling (Fig. 13). Therefore, further experiments are required to address the potential role of PARP16 and ABL2 on ISR-driven IRE1 activation. Previous work by Wiseman et al (2010) found that the flavonol quercetin could activate yeast Ire1 by binding to the cytosolic kinase domain, so it is also possible that the presence of a metabolite could also activate IRE1.

In summary, we have found that the ISR mediates IRE1 activation driven by its cytosolic domain. While the exact trigger remains unclear, it is downstream of eIF2α phosphorylation, but independent of the canonical ISR transcriptional response dependent on ATF4, CHOP, etc.

What is the purpose of the selective activation of IRE1 in response to eIF2α phosphorylation (Fig. 11)? On one hand, IRE1 degrades DR5 mRNA upon activation (Lu et al, 2014 and Fig. 10) and therefore, it is tempting to speculate that IRE1 activation could be cytoprotective not just in the UPR but also in the ISR. On the other hand, we cannot exclude the possibility that ISR-driven IRE1 activation leads to TRAF2 mediated apoptosis and inflammatory responses (Nishitoh et al, 2002). Furthermore, the transcription factor XBP1s targets many genes involved in multiple cellular functions (Acosta-Alvear et al, 2007). Since transcription programs activated by XBP1s upon ER stress and lipid dysregulation are different (Koh et al, 2018; Ho et al, 2020), it is tempting to speculate that the ISR might trigger yet a third XBP1-driven transcription program. Further experiments will be required to test this hypothesis, which will depend on identifying ways to prevent ISR driven IRE1 activation.

There are different models that explain how IRE1 gets activated (reviewed in Adams et al, 2019). Our observations indicating that IRE1 activation is independent of protein folding- and lipid bilayer-stress suggest that IRE1 activation could occur on the cytosolic face of the ER membrane.

CHAPTER 4. Summary and future perspectives

In this work, we (1) define that the four different eIF2α kinases share a common cell-autonomous apoptosis pathway that culminates in the induction of DR5 downstream eIF2α, (2) showcase a synthetic biology approach to activate the ISR in the absence of stress, allowing us to decouple the stress sensing from downstream effects, and (3) describe a new layer of interconnectivity between the ISR and UPR. Our research demonstrates that the ISR engages DR5, an otherwise plasma membrane-localized cell death receptor, to signal unconventionally, from within the Golgi apparatus. Surprisingly, stress-free ISR signaling also activated the ER stress sensor IRE1 in the absence of ER stress, suggesting putative cytosolic activation of IRE1.

Together, our results support a model in which a fundamental part of the ISR is to actuate a common cell death mechanism in charge of eliminating terminally injured cells which can no longer cope with or adapt to stress, thereby preserving tissues and organs. Furthermore, the ISR modulates the activation of the UPR through IRE1, opening new door to a better understanding of the molecular mechanisms linking the ISR to other cellular processes to regulate homeostasis.

In light of these findings, it will be important to assess how ISR-driven IRE1 activation occurs and its potential roles in maintaining cellular homeostasis. There are several potential mechanisms by which the ISR may activate IRE1. For example, sustained ISR signaling could activate a cytosolic protein that stimulates IRE1 function. A candidate approach aimed at dissecting the roles of PARP16 or ABL-2 in ISR-driven IRE1 activation may reveal a potential mechanism. Since eIF2α

phosphorylation leads to protein synthesis inhibition, it would be interesting to study whether blocking or reducing translation using pharmacological protein synthesis inhibitors, such as cycloheximide or puromycin leads to IRE1 activation. If this is the case, then it is conceivable that IRE1 may moonlight as a sentinel of protein synthesis.

Further studies are also required to determine how DR5 is activated by the ISR. The bulk of DR5 localizes to the Golgi apparatus upon activation of the ISR, even in the absence of stress, indicating that the accumulation of DR5 in the Golgi apparatus is intrinsic to the ISR and not necessarily dependent on stresses that could potentially alter the secretory pathway. As mentioned earlier, considering that some misfolded proteins bind DR5, it remains plausible that a sustained ISR may induce the accumulation of a single or a subset of select ER client protein(s) that may engage DR5 leading to its activation. Coupled RNAseq and proteomics in cells in which we activate the ISR synthetically may shed light on the mechanism of activation of DR5 during the terminal ISR.

Cellular stress responses are fundamental for normal physiology and their dysregulation has been linked to many common human diseases (Mouton-Liger et al, 2012; Ma et al, 2013; Hoozemans et al, 2007; Zhu et al, 2019). Therefore, a better understanding of elemental molecular mechanisms governing cellular stress responses promises to guide the development of new therapeutic interventions for the betterment of human health.

CHAPTER 5. Materials and Methods

Plasmid construction, genetic knockdown and generation of stable cell lines

H4 cells expressing the CRISPRi machinery (Gilbert et al, 2014) were a kind gift from Martin Kampmann (UCSF). DR5, ATF4, and ATF6 and PKR genes were depleted using CRISPRi as previously described (Gilbert et al, 2014). Briefly, CRISPRi cells were transduced with VSV-G pseudotyped lentiviruses harboring the three top small guide RNAs (DR5: 5'-GGGCAAGACGCACCAGTCGT-3'; 5'-GAGAGATGGGTCCCCGGGTT-3'; 5'-GAAAGTAGATCGGGCATCGT-3') (ATF4: 5'-GGACGAAGTCTATAAAGGGC-3'; 5'-GCATGGCGTGAGTACCGGGG-3'; 5'-GGCTGTTGCCCCACGAAACG-3') (ATF6: 5'-GTTAATATCTGGGACGGCGG-3'; 5'-GTATTAATCACGGAGTTCCA-3'; 5'-GCCACGAGTGGGCGGAAGTA-3') (PKR: 5'-GGCCGCCGGCCGGAGACCCG-3'; 5'-GGCGGCGGCGCAGGTGAGCA-3'; 5'-GGAAGCCGCGGGTCTCCGGC-3'). The sgRNA sequences were obtained from the human genome-scale CRISPRi library developed by the laboratory of Jonathan Weissman (MIT, Whitehead Institute).

FKBP-PKR was generated by cloning a PCRP encoding residues 170-551 of PKR of human origin obtained using oligonucleotides containing a 5'-BamHI site and a 3' FLAG-epitope coding sequence and MfeI sites into the cognate sites of p1XDmrB-mCh-LRP6c (kind gift of Peter Walter). The resulting construct, pDAA-006, replaces the mCh-LRP6c coding sequences in p1XDmrB-mCh-LRP6c with the abovementioned PKR coding sequence. The FLAG-epitope tagged FKBP-PKR coding sequence was excised from pDAA-006 with XhoI and MfeI and subcloned into

the XhoI and EcoRI sites of pLPCX-IRES-eGFP. pLPCX-IRES-eGFP was generated by cloning a fusion PCRP consisting of the encephalomyocarditis virus internal ribosomal entry site (EMCV-IRES) upstream of the eGFP coding sequence flanked by EcoRI and NotI sites into the cognate sites of pLPCX (Clontech). eIF2-alpha S51D was generated by cloning of a PCRP encoding the eIF2-alpha S51D coding sequence into the pENTREGFP2 (Addgene #2245) to generate pFBK001. eIF2-alpha S51D was a kind gift from David Ron (University of Cambridge, UK). U2OS IRE1α KO cell line (parental cell line, ATCC) was a kind gift from Peter Walter (UCSF). The plasmid encoding pGpHUSH IRE1α ΔLD GFP was constructed by insertion of a PCRP encoding GFP tagged human IRE1 deleted of its luminal domain into the lentiviral vector pGpHUSH.puro (Genentech) (Li et al, 2010). The point mutant of the IRE1α ΔLD coding sequence was generated by site-directed mutagenesis of the corresponding expression construct.

Stable cell lines bearing transgenes were generated by retroviral transduction as previously described (Sidrauski et al, 2013). Briefly, VSV-G pseudotyped retroviral particles encoding constructs of choice were prepared using standard protocols using GP2-293 packaging cells (Clontech). Viral supernatants were collected and used to infect target cells by centrifugal inoculation (spinoculation). For retroviral infections, target cells were plated at a density of 2×10^5 cells/well in 6-well plates one day before transduction in presence of 8 µg/ml polybrene. Pseudoclonal cell populations were obtained by fluorescence-activated cell sorting using a narrow gate placed over the mean of the signal distribution as previously described (Zappa et al, 2022).

Cell culture, transfection, and drug treatments

H4 cells, HEK293 cells, and U2OS cells were maintained in in Dulbecco's Modified Eagle Medium (DMEM) supplemented with 10% fetal bovine serum (FBS) and penicillin/streptomycin at 37°C, 5% CO2 in a humidified incubator. For data collection, cells were seeded at a density of 1-2 × 10^5 cells/well in 6-well plates, 0.7-1.0 × 10^5 cells/well in 12-well plates, or 0.5-0.7 × 10^5 cells/well in 24-well plates and maintained for a further 24 h before any treatment. Cells were treated with ISR stress inducers 300 nM thapsigargin (Sigma-Aldrich), 3 μM oligomycin (Sigma-Aldrich), 5 mM histidinol (Sigma-Aldrich), or transfected with 250 nM poly I:C (Tocris), as previously described (Zappa et al, 2022), 1μM ISRIB (Sigma-Aldrich), 50 μM Z-VAD-FMK (SelleckChem), or 1 μg/ml FcDR5 (R&D systems) as indicated. FKBP-PKR was activated with 100 nM of the homodimerization ligand AP20187 (Takara), as previously described (Zappa et al, 2022). For IRE1α and ATF6 10 μM 4μ8c (Sigma-Aldrich) and 5 μM ceapin (Sigma-Aldrich) were used, respectively.

ATF3, ATF4, ATF5 and CHOP gene silencing was obtained through transfection of synthetic small interfering RNA (siRNA). Depletion of each gene was performed using a pool of synthetic small interfering RNAs (ATF3: Dharmacon siGenomeSMART pool; 5'-CUGGGUCACUGGUGUUUGATT -3', 5'-GCAAAGUGCCGAAACAAGATT -3' and 5'-GGAGGACUCCAGAAGAUGATT -3' and their reverse complements targeting gene NM_001030287.4), (ATF4: Dharmacon siGenomeSMART pool; 5'-GUGAGAAACUGGAUAAGAATT -3', 5'- GCCUAGGUCUCUUAGAUGATT-3' and 5'-CCCUGUUGGGUAUAGAUGATT -3' and their reverse complements targeting gene NM_001675.4), (ATF5: Dharmacon siGenomeSMART pool; 5'-

GAAUCGCGAGCUGAAGGAATT -3', 5'- UGAGCGAGUUGAUUUCACATT-3' and 5'-CGCGAGAUCCAGUACGUCATT -3' and their reverse complements targeting gene NM_001193646.2), (CHOP: Dharmacon siGenomeSMART pool; 5'-GGAAGAACUAGGAAACGGA -3'and 5'- CAGUAUCUUGAGUCUAAUATT -3' and 5'-CUGGGAAACAGCGCAUGAA-3' and their reverse complements targeting gene NM_019843) transfected with Lipofectamine 2000 following the manufacturer's recommendations. All RNAi experiments were carried out at 96 h after transfection. recommendations.

Immunoblotting

Cell lysates were obtained by collecting cells directly in Laemmli SDS-PAGE sample buffer (62.5 mM Tris-HCl pH 6.8, 2% SDS, 10% glycerol and 0.01% bromophenol blue). Lysates were briefly sonicated and supplemented with fresh 5% 2-mercaptoethanol prior to heat denaturation and separation by SDS-PAGE. Lysates were separated 8-10% SDS-PAGE gels and transferred onto nitrocellulose membranes for immunoblotting. Immunoreactive bands were detected by enhanced chemiluminescence using horse radish peroxidase (HRP)-conjugated secondary antibodies. The antibodies and dilutions used were as follows: PKR (Cell Signaling Technology 3072, 1:2000), phospho-PKR (T466) (Abcam AB322036, 1:2000), eIF2α (Cell Signaling Technology 9722, 1:1000), phospho-eIF2α (Cell Signaling Technology 9721, 1:1000), FLAG (M2 clone Sigma Aldrich F1804, 1:2000), ATF4 (Cell Signaling Technology 11815, 1:1000), CHOP (Cell Signaling Technology 2895, 1:1000), DR5 (Cell Signaling Technology 8074, 1:1000), PARP1(Cell Signaling 9532, 1:1000), caspase-8 (Cell Signaling Technology 9746, 1:1000) caspase-3 (Cell Signaling

Technology 9662, 1:1000), IRE1α (Cell Signaling 3294, 1:1000), phospho-IRE1α (Novus MB100-2323), PERK (Cell Signaling 5683, 1:1000), Puromycin (Millipore MABE343, 1:1000), β-actin (1:5000, Sigma Aldrich, 061M4808), anti-GAPDH (Abcam 8245, 1:5000,), all diluted in 1% BSA-TBST. Secondary anti-rabbit and anti-mouse HRP-conjugated antibodies (Cell Signaling Technology 7074, 7076) were used at 1:5000 dilutions in 1% BSA-TBST.

Immunofluorescence analyses

H4 cells were grown on coverslips in 24-well plates, fixed with 4% PFA for 10 min, washed three times with PBS, and permeabilized with blocking solution (0.05% saponin, 0.5% BSA, 50 mM, NH4Cl in PBS) for 20 min. DR5 (Cell Signaling Technology 8074, 1:200) and GM130 (BD technology 610822, 1:1000) primary antibodies were diluted in blocking solution and incubated for 1 hour at room temperature. The coverslips were washed with PBS and incubated with fluorochrome-conjugated secondary antibodies (Alexa fluor anti-mouse 647; Invitrogen A32728 and Alexa fluor anti-rabbit 568; Invitrogen A11011 diluted at 1:500 dilution in blocking solution) and DAPI (0.1 µg/mL) for 45 minutes at RT. Fixed cells were washed 2 times in PBS and one time in ddH_2O and mounted on coverslips with Mowiol. Imaged were acquired using a resonant scanning confocal microscope (Leica SP8) equipped with a Plan Apochromat 60 × NA 1.2 oil immersion objective. Fluorescence microscopy images were processed with Fiji (ImageJ: National Institutes of Health) software. To determine the proportion of DR5 in the *cis*-Golgi complex, each cell in the field of view was cropped and a single ROI was drawn manually to quantify the total DR5 fluorescence signal. GM130 signal was used to calculate the DR5 signal in the *cis*-

Golgi complex using the Fiji plug-in “create selection”. An average of 200 cells per time point was considered for each replicate. The data were expressed as the ratio between DR5 MFI in the cis-Golgi compartment over the total DR5 MFI. Statistical significance for differences between groups was calculated using the unpaired Student’s t-test with the GraphPad Prism software. All data reported as mean ± s.e.m.

Cell viability assays

To measure cell viability by flow cytometry, we collected detached cells and adherent cells. Detached cells were first collected by centrifugation. Adherent cells were collected by trypsinization. Both cell populations were pooled and resuspended in PBS supplemented with 2% FBS and 0.1 mg/ml RNase. Subsequently, propidium iodide (PI, 1.5 µg/ml) was added to the cell suspension. The samples were incubated on ice for 10 min and separated in an Attune cytPix flow cytometer. Flow cytometry data was analyzed using FlowJo (TreeStar, USA). The proportions of live and dead cells as determined by PI staining were used as cell viability metrics.

DR5 neutralizing antibody assay

Cells bearing FKBP-PKR cells were washed 2 times with PBS and either fresh cell culture medium (control) or fresh cell culture medium supplemented with FcDR5 neutralizing antibody (1 µg/ml) overnight. The following day, 100 nM of the homodimerization ligand AP20187 was added to the cells and the cells were incubated for 24 hours prior to collection for analysis by immunoblotting or flow cytometry.

Puromycilation of nascent peptides

Puromycilation of nascent peptides was performed as described (Zappa et al, 2019). Briefly, 2 × 10^5 FKBP-PKR cells were grown in 6-well plates and the AP20187 homodimerizer was added 24 hours after. 9 µM puromycin (PMY) was added one hour after addition of AP20187. Cells were incubated with PMY for 20 min at 37°C before sample collection. The cells were collected and analyzed as described for Immunoblotting.

RNA sequencing

RNA-Seq library was generated using RNA isolated fom FKBP-PKR expressing cells after 4, 12 and 18 h of homodimerizer treatment using NEBNext Ultra II Library Prep Kit. The mRNA was enriched by oligo-dT pulldown from total RNA, followed by fragmentation, adapter ligation, PCR amplification. The library was then sequenced using Illumina HiSeq 4000 Single-End 50bp (SE50). Cutadapt was used to filter transcripts below 20 nucleotides and remove adapters. FastQC was used to validate the quality of trimmed and filtered reads. Sequencing reads were then mapped to the hg38 human genome using Kallisto set to map unpaired reads with default parameters and the transcript abundance output files were analyzed using Deseq2. Deseq2 was used to assess differentially expressed genes (DEGs) between groups [q (p-value corrected for false discovery rate, FDR) < 0.05 and fold change > 1.5 or < -1.5). Default thresholds of Deseq2 were used to identify DEGs. We then used the package pheatmap of R to generate the heatmap based on this TPM (transcripts per million) matrix. GSEA analyses were conducted with GSEA v4.0.3. Normalized abundance

files produced by Deseq2 were used as inputs for GSEA. GSEA analysis was conducted for Hallmark (GSEA specific ontology database) and KEGG pathways separately.

RNA extraction, CDNA synthesis and qRT-PCR Analysis

Total RNA from sub-confluent H4 cells was isolated using the RNeasy RNA purification kit (Qiagen), following the manufacturer's recommendations. 1 µg to total RNA was reverse transcribed with SuperScript VILO (Invitrogen) the manufacturer's recommendations. The resulting cDNA was used as a template for real-time qPCR using PowerUp SYBR Green Master Mix (Applied Biosystems), according to the manufactures's protocol. GAPDH or β-ACTIN were used as normalizing controls to estimate fold-change in mRNA expression. Semi quantitative PCRs were performed using cDNA templates, Taq Polymerase (NEB), and the same primers as for qRT-PCR (see Materials). Reactions were separated on TAE agarose gels. Oligonucleotide primers used in this study are provided in Table S1.

Table S1

Target	5'-3'Primer sequence (Fwd)	5'-3' Primer sequence (Rev)
DR5	CCAGCAAATGAAGGTGATCC	CGGTTTTGTTGACCCACTTT
DR4	TGAAGGGTCTCAGAGGAGGA	CCATTTCATCAGCATTGCAT
TRAIL	CACATAACTGGGACCAGAGGA	CCTGAAATCGAAAGTATGTTTGG'

GADD34	TGAGGCAGCCGGAGATAC	GTAGCCTGATGGGGTGCTT
CHOP	TTAAGTCTAAGGCACTGAGCGTATC	TGCTTTCAGGTGTGGTGATG
XBP1 u/s	GGAGTTAAGACABCGCTTGG	ACTGGGTCCAAGTTGTCCAGAGCT
SCARA3	CCGAAGACATCTCCTTGACC	CAGTTCTGAATTCCCTCCA
Col6A1	CTGGGCGTCAAAGTCTTCTC	ATTCGAAGGAGCAGCACACT
BLOSC1	AGCTGGACCATGAGGTGAAG	CTGCAGCTGCCCTTTGTAG
HSPA5	TGCAGCAGGACATCAAGTTC	AGTTCCAGCGTCTTTGGTTG
GRP-94	TCCAATTCAAGGTAATCAGAT	CCAGTTTGGTGTCGGTTTCT’
DNAJB9	CGGATGCTGAAGCAAAATTC	TTCTTGGATCCAGTGTTTTGG
β-ACTIN	TTCTACAATGAGCTGCGTGTG	AGGGCATACCCCTCGTAGAT
GAPDH	AGCCACATCGTCCAGACAC	TGGAAGATGGTGATGGGATT
28S	AAACTCTGGTGGAGGTCCGT	CTTACCAAAAGTGGCCCACTA

References

Acosta-Alvear D, Zhou Y, Blais A, Tsikitis M, Lents NH, Arias C, Lennon CJ, Kluger Y & Dynlacht BD (2007) XBP1 controls diverse cell type- and condition specific transcriptional regulatory networks. Mol Cell 27, 53-66.

Acosta-Alvear D, Karagöz GE, Fröhlich F, Li H, Walther TC & Walter P (2018) The unfolded protein response and endoplasmic reticulum. protein targeting machineries converge on the stress sensor IRE1 *eLife* 7:e43036

Adams CJ, Kopp MC, Larburu Na, Nowak PR & Ali Maruf MU (2019) Structure and Molecular Mechanism of ER Stress Signaling by the Unfolded Protein Response Signal Activator IRE1.Front. Mol. Biosci., 6.

Adomavicius T, Guaita M, Zhou Y, Jennings MD, Latif Z, Roseman AM & Pavitt GD (2019) The structural basis of translational control by eIF2 phosphorylation. Nat Commun 10: 2136.

Balachandran S, Roberts PC, Brown LE, Truong H, Pattnaik AK, Archer DR & Barber GN (2000) Essential Role for the dsRNA-Dependent Protein Kinase PKR in Innate Immunity to Viral Infection. Immunity13:129–141.

Baltzis D., Li S., & Koromilas AE (2002) Functional characterization of PKR gene products expressed in cells from mice with a targeted deletion of the N terminus or C terminus domain of PKR. Journal of Biological Chemistry,277(41), 38364-38372. doi:10.1074/jbc.m203564200.

Bando Y, Onuki R, Katayama T, Manabe T, Kudo T, Taira K & Tohyama M (2005) Double strand RNA dependent protein kinase (PKR) is involved in the extrastriatal degeneration in Parkinson's disease and Huntington's disease. Neurochem Int 46: 11–18.

Bertolotti A, Zhang Y, Hendershot LM, Harding HP &Ron D (2000) Dynamic interaction of BiP and ER stress transducers in the unfolded-protein response. Nat Cell Biol. 2:326–332. doi:10.1038/3501401.

Berlanga JJ, Herrero S & de Haro C (1998) Characterization of the hemin-sensitive eukaryotic initiation factor 2alpha kinase from mouse nonerythroid cells. J Biol Chem 273: 32340–32346.

Besch R, Poeck H, Hohenauer T, Senft D, Häcker G, Berking C, Hornung V, Endres S, Ruzicka T, Rothenfusser S, et al (2009) Proapoptotic signaling induced by RIG-I and MDA-5 results in type I interferon–independent apoptosis in human melanoma cells. J Clin Invest 119: 2399–2411.

Billen LP, Kokoski CL, Lovell JF, Leber B & Andrews DW (2008) Bcl-XL inhibits membrane permeabilization by competing with Bax. PLoS Biol 6:e147.

Bond S, Lopez-Lloreda C, Gannon PJ, Akay-Espinoza C & Jordan-Sciutto KL (2020) The Integrated Stress Response and Phosphorylated Eukaryotic Initiation Factor 2α in Neurodegeneration. J Neuropathol Exp Neurol 79: 123–143.

Buchman TG (2002) The community of the self. Nature 420:246–251.

Calfon M, Zeng H, urano F, Till JH, Hubbard SR, Harding HP, et al (2002) IRE1 couples endoplasmic reticulum load to secretory capacity by processing the XBP-1 mRNA. *Nature* 415, 92-96. Doi: 10.1038/415092a.

Castelli JC, Hassel BA, Maran A, Paranjape J, Hewitt JA, Li X, Hsu Y-T, Silverman RH & Youle RJ (1998) The role of 2′-5′ oligoadenylate-activated ribonuclease L in apoptosis. Cell Death Differ 5: 313–320.

Castilho BA, Shanmugam R, Silva RC, Ramesh R, Himme BM & Sattlegger E (2014) Keeping eta eIF2 alpha kinase Gcn2 in check. Biochim Biophys Acta 1843:1948-1968.

Chen JJ, Throop MS, Gehrke L, Kuo I, Pal JK, Brodsky M & London IM (1991) Cloning of the cDNA of the heme-regulated eukaryotic initiation factor 2 alpha (eIF-2 alpha) kinase of rabbit reticulocytes: homology to yeast GCN2 protein kinase and human double-stranded-RNA-dependent eIF-2 alpha kinase. Proc Natl Acad Sci USA 88: 7729–7733.

Chen JJ (2014) Translational control by heme-regulated eIF2α kinase during erythropoiesis. Curr. Opin. Hematol 21, 172–178.

Chen I (2019) An antisense oligonucleotide splicing modulator to treat spinal muscular atrophy. Nature Research.

Clackson T, Yang W, Rozamus LW, Hatada M, Amara JF, Rollins CT, Stevenson LF, Magari SR, Wood SA, Courage NL, Lu X, Cerasoli F, Gilman M & Holt DA (1998) Redesigning an FKBP-ligand interface to generate chemical dimerizers with novel specificity. Proceedings of the National Academy of Sciences. 95:10437–10442. doi:10.1073/pnas.95.18.10437.

Costa-Mattioli M & Walter P (2020) The integrated stress response: From mechanism to disease. Science 368: eaat5314.

Cox JS, Shamu CE & Walter P (1993) Transcriptional induction of genes encoding endoplasmic reticulum resident proteins requires a transmembrane protein kinase. Cell 73, 1197-1206. Doi: 10.1016/0092-8674(93)90648-A.

Cox JS & Walter P (1996) A novel mechanism for regulating activity of a transcription factor that controls the unfolded protein response. Cell 87, 391-404. Doi: 10.1016/S0092-8674(00)81369-4.

Dar AC, Dever TE, & Sicheri F (2005) Higher-Order Substrate Recognition of eIF2α by the RNA-Dependent Protein Kinase PKR. Cell. 122:887–900. doi:10.1016/j.cell.2005.06.044.

Deng J, Harding HP, Raught B, Gingras AC, Berlanga JJ, Scheuner D, Kaufman RJ, Ron D & Sonenberg N (2002) Activation of GCN2 in UV-irradiated cells inhibits translation. Curr Biol 12:1279-1286.

Dey M, Cao C, Dar AC, Tamura T, Ozato K, Sicheri F, & Dever TE (2005) Mechanistic Link between PKR Dimerization, Autophosphorylation, and eIF2α Substrate Recognition. Cell. 122:901–913. doi:10.1016/j.cell.2005.06.041.

Dong J, Qiu H, Garcia-Barrio M, Anderson J & Hinnebus h AG (2000) Uncharged tRNA activates GCN2 by displacing the protein kinase moiety from a bipartite tRNA-binding domain. Mol Cell 6: 269–279.

Ehrenfeld E & Hunt T (1971) Double-Stranded Poliovirus RNA Inhibits Initiation of Protein Synthesis by Reticulocyte Lysates. Proceedings of the National Academy of Sciences 68:1075–1078.

Eiermann N, Haneke K, Sun Z, Stoecklin G & Ruggieri A (2020) Dance with the Devil: Stress Granules and Signaling in Antiviral Responses. Viruses. 12.

Elbarbary RA, Li W, Tian B & Maquat LE (2013) STAU1 binding 3′ UTR IRAlus complements nuclear retention to protect cells from PKR-mediated translational shutdown. Genes Dev 27: 1495–1510.

English AM, Green KM & Moon SL (2021) A (dis)integrated stress response: Genetic diseases of eIF2α regulators. Wiley Interdiscip Rev RNA. (3):e1689. doi: 10.1002/wrna.1689. Epub. PMID: 34463036.

Elouil H, Bensellam M, Guiot Y, Vander Mierde D, Pascal SM, Schuit FC & Jonas JC. (2007) Acute nutrient regulation of the unfolded protein response and integrated stress response in cultured rat pancreatic islets. Diabetologia. 50(7):1442-52. doi: 10.1007/s00125-007-0674-4. Epub 2007 May 12. PMID: 17497122.

Fuchs Y & Steller H (2015) Live to die another way: modes of programmed cell death and the signals emanating from dying cells. *Nat. Rev. Mol. Cell Biol.* 16, 329–344.

Fulda S & Debatin K-M (2006) Extrinsic versus intrinsic apoptosis pathways in anticancer chemotherapy. Oncogene 25: 4798–4811.

Fulda S, Gorman AM, Hori O & Afshin Samali A (2010) Cellular Stress Responses: Cell Survival and Cell Death. International Journal of Cell Biology, vol 2010. ID 214074, 23 pages.

Gal-Ben-Ari S, Barrera I, Ehrlich M & Rosenblum K (2019) A Kinase to Remember. Front Mol Neurosci 11.

Gallagher CM & Walter P (2016) Ceapins inhibit ATF6α signaling by selectively preventing transport of ATF6α to the Golgi apparatus during ER stress. *eLife* 5:e11880.

Gales L (2019) Tegsedi (Inotersen): An Antisense Oligonucleotide Approved for the Treatment of Adult Patients with Hereditary Transthyretin Amyloidosis. Pharmaceuticals (Basel) 12: E78.

Galluzzi L, Yamazaki T & Kroemer G (2018) Linking cellular stress responses to systemic homeostasis. *Nat Rev Mol Cell Biol* 19, 731–745. https://doi.org/10.1038/s41580-018-0068-0.

Gardner BM & Walter P (2011) Unfolded proteins are Ire1-activating ligands that directly induce the unfolded protein response. *Science* 333, 1891-1894. Doi: 10.1126/science.1209126.

Gilbert LA, Larson M, Morsut L, Liu Z, Brar G, Torres S, Stern-Ginossar N, Brandman O, Whitehead EH, Doudna JA, Lim W A, Weissman JS & Qi L (2013) CRISPR-Mediated Modular RNA-Guided Regulation of Transcription in Eukaryotes. Cell,154(2), 442-451. doi:10.1016/j.cell.2013.06.044

Gilbert LA, Horlbeck MA, Adamson B, Villalta JE, Chen Y, Whitehead EH, Guimaraes C, Panning B, Ploegh HL, Bassik MC, et al (2014) Genome-Scale CRISPR-Mediated Control of Gene Repression and Activation. Cell 159: 647–661.

Grimm, D. (2011) The dose can make the poison: lessons learned from adverse in vivo toxicities caused by RNAi overexpression. Silence 2:8.

Guo X, Aviles G, Liu Y, Tian R, Unger BA, Lin YHT, Wiita AP, Xu K, Correia MA & Kampmann M (2020) Mitochondrial stress is relayed to the cytosol by an OMA1-DELE1-HRI pathway. Nature 579: 427–432.

Halbleib K, Pesek K, Covino R, Hofbauer H, Wunnicke D, Hänelt I, Hummer G & Ernst R (2017) Activation of the Unfolded Protein Response by Lipid Bilayer Stress. Molecular Cell, 67(4), pp.673-684.e8.

Halliday M, Radford H, Sekine Y, Moreno J, Verity N, le Quesne J, Ortori CA, Barrett DA, Fromont C, Fischer PM, et al (2015) Partial restoration of protein synthesis rates by the small molecule ISRIB prevents neurodegeneration without pancreatic toxicity. Cell Death Dis 6: e1672–e1672.

Han AP, Yu C, Lu L, Fujiwara Y, Browne C, Chin G, Fleming M, Leboulch P, Orkin SH & Chen JJ (2001) Heme-regulated eIF2alpha kinase (HRI) is required for translational regulation and survival of erythroid precursors in iron deficiency. EMBO J 20: 6909–6918.

Harding H, Zhang Y & Ron D (1999) Protein translation and folding are coupled by an endoplasmic-reticulum-resident kinase. Nature, 397(6716), pp.271-274.

Harding HP, Ordonez A, Allen F, Parts L, Inglis AJ, Williams RL & Ron D (2019) The ribosomal P-stalk couples amino acid starvation to GCN2 activation in mammalian cells. eLife 8: e50149.

Harding P, Zhang Y, Bertolotti A, Zeng H & Ron D (2000) Perk Is Essential for Translational Regulation and Cell Survival during the Unfolded Protein Response. Molecular Cell 5: 897–904.

Hetz C (2012) Unfolded protein response: controlling cell fate decisions under ER stress and beyond Nat. Rev. Mol. Cell Biol.,13, pp.89-102.

Hetz C, Zhang K, & Kaufman RJ (2020) Mechanisms, regulation and functions of the unfolded protein response. Nature Reviews Molecular Cell Biology, 21(8), 421–438.

Hillary RF & FitzGerald UA (2018) lifetime of stress: ATF6 in development and homeostasis. *J Biomed Sci* 25, 48.

Hinnebusch AG, Ivanov IP & Sonenberg N (2016) Translational control by 5’-untranslated regions of eukaryotic mRNAs. Science 352: 1413–1416.

Hirota M, Kitagaki M, Itagaki Hb & Aiba S (2006) Quantitative measurement of spliced XBP1 mRNA as an indicator of endoplasmic reticulum stress. J Toxicol Sci.31(2):149-56. doi: 10.2131/jts.31.149. PMID: 16772704.

Ho N, Yap WS, Xu J, Wu H, Koh JH, Goh WWB, George B, Chong SC, Taubert S & Thibault G (2020) Stress sensor Ire1 deploys a divergent transcriptional program in response to lipid bilayer stress. J Cell Biol 219.

Hoozemans JJ et al (2007) Activation of the unfolded protein response in Parkinson's disease. Biochem. Biophys. Res. Commun 354, 707–711. doi: 10.1016/j.bbrc.2007.01043.

Ill-Raga G, Tajes M, Busquets-Garcia A, Ramos-Fernandez E, Vargas LM, Bosch-Morato M, Guivernau B, Valls-Comamala V, Eraso-Pichot A, Guix FX, et al (2015) Physiological control of nitric oxide in neuronal BACE1 translation by heme-regulates eIF2alpha kinase HRI induces synaptogenesis. Antioxid Redox Signal 22: 1295-1307.

Inglis AJ et al (2019) Activation of GCN2 by the ribosomal P-stalk. Proc. Natl. Acad. Sci. U.S.A 116, 4946–4954.

Jwa M & Chang P. (2012) PARP16 is a tail-anchored endoplasmic reticulum protein required for the PERK- and IRE1α-mediated unfolded protein response. Nat Cell Biol. (11):1223-30.

Kang R & Tang D (2012) PKR-dependent inflammatory signals. Sci Signal. 5(247):pe47. doi: 10.1126/scisignal.2003511. PMID: 23092889; PMCID: PMC3656404.

Karagöz GE, Acosta-Alvear D, Nguyen HT, Lee CP, Chu F, & Walter P (2017) An unfolded protein-induced conformational switch activates mammalian IRE1. eLife 6.

Karagöz GE, Aragón T & Acosta-Alvear D. Recent advances in signal integration mechanisms in the unfolded protein response [version 1; peer review: 2 approved] F1000Research 2019, 8 (F1000 Faculty Rev):1840 (https://doi.org/10.12688/f1000research.19848.1).

Khan SF (2021) Homeostasis: Definition, types and examples. *PhD Nest.* Last updated: Sept. 30, 2021. https://www.phdnest.com/homeostasis-definition-types-and-examples/.

Kim Y, Lee JH, Park J-E, Cho J, Yi H & Kim VN (2014) PKR is activated by cellular dsRNAs during mitosis and acts as a mitotic regulator. Genes Dev 28: 1310–1322.

Kim Y, Park J, Kim S, Kim M, Kang M-G, Kwak C, Kang M, Kim B, Rhee H-W & Kim VN (2018) PKR Senses Nuclear and Mitochondrial Signals by Interacting with Endogenous Double-Stranded RNAs. Mol Cell 71: 1051–1063.e6.

Koh JH, Wang L, Beaudoin-Chabot C & Thibault G (2018) Lipid bilayer stress-activated IRE-1 modulates autophagy during endoplasmic reticulum stress. J. Cell Sci. 131 jcs217992 10.1242/jcs.217992.

Korsmeyer SJ, Wei MC, Saito M, Weiler S, Oh KJ & Schlesinger PH (2000) Pro-apoptotic cascade activates BID, which oligomerizes BAK or BAX into pores that result in the release of cytochrome c. Cell Death Differ 7: 1166–1173.

Krukowski K, Nolan A, Frias ES, Boone M, Ureta G, Grue K, Paladini M-S, Elizarraras E, Delgado L, Bernales S, et al (2020) Small molecule cognitive enhancer reverses age-related memory decline in mice. eLife 9: e62048.

Lam M, Marsters SA, Ashkenazi A & Walter P (2020) Misfolded proteins bind and activate death receptor 5 to trigger apoptosis during unresolved endoplasmic reticulum stress. Elife 9: e52291.

Leber JH, Bernales S & WaterP (2004) IRE1-independent gain control of the unfolded protein response. PLoS Biol. 2e235 10.137/journal.pbio.0020235.

Lei K & Davis RJ (2003) JNK phospohorylation of Bim-relates members of the Bcl2 family induces Bax-dependent apoptosis. Proc. Natl. Acad. Sci. U. S. A. 100:2432-2437)

Lemaire PA, Lary J, & Cole JL (2005) Mechanism of PKR activation: dimerization and kinase activation in the absence of double-stranded RNA. J Mol Biol. 345:81–90.

Lemaire PA, Anderson E, Lary J & Cole JL (2008) Mechanism of PKR Activation by dsRNA,J Mol Biol. 381:351-360,ISSN 0022-2836.

Li S, Peters GA, Ding K, Zhang X Qin J & Sen GC (2006) Molecular basis for PKR activation by PACT or dsRNA. *Proc. Natl. Acad*. Sci. U.S.A. 103, 10005-10010. Soi: 10.1073/pnas.0602317103.

Li H, Korennykh AV, Behrman SL & Walter P (2010) Mammalian endoplasmic reticulum stress sensor IRE1 signals by dynamic clustering. Proc Natl Acad Sci U S A. 107(37):16113-8. doi: 10.1073/pnas.1010580107. Epub 2010 Aug 26. PMID: 20798350; PMCID: PMC2941319.

Li L, Tan H, Gu Z, Liu Z, Geng Y, Liu Y, Tong H, Tang Y, Qiu J & Su L (2014) Heat stress induces apoptosis through a Ca^{2+}-mediated mitochondrial apoptotic pathway in human umbilical vein endothelial cells. PLoS One. 9(12):e111083. doi: 10.1371/journal.pone.0111083. PMID: 25549352; PMCID: PMC4280109.

Lu M, Lawrence DA, Marsters S, Acosta-Alvear D, Kimmig P, Mendez AS, Paton AW, Paton JC, Walter P & Ashkenazi A (2014) Opposing unfolded-protein-response signals converge on death receptor 5 to control apoptosis. Science 345: 98–101.

Ma T et al (2013) Suppression of eIF2α kinases alleviates Alzheimer's disease-related plasticity and memory deficits. Nat. Neurosci. 16, 1299–1305 doi: 10.1038/nn.3486.

Marciniak SJ, Garcia-Bonilla L, Hu J, Harding HP & Ron D. (2006) Activation-dependent substrate recruitment by the eukaryotic translation initiation factor 2 kinase PERK. 172, 201-209.

McCartney S, Vermi W, Gilfillan S, Cella M, Murphy TL, Schreiber RD, Murphy KM & Colonna M (2009) Distinct and complementary functions of MDA5 and TLR3 in poly(I:C)-mediated activation of mouse NK cells. J Exp Med. 206(13):2967-76. doi: 10.1084/jem.20091181. Epub 2009 Dec 7. PMID: 19995959; PMCID: PMC2806445.

McEwen E, Kedersha N, Song B, Scheuner D, Gilks N, Han A, Chen JJ, Anderson P & Kaufman RJ (2005) Heme-regulated inhibitor kinase-mediated phosphorylation of eukaryotic translation initiation factor 2 inhibits translation, induces stress granule formation, and mediates survival upon arsenite exposure. J Biol Chem 280: 16925-16933.

MeursE, Chong K, Galabru J, Thomas NS, Kerr IM, Williams BR & Hovanessian AG (1990) Molecular cloning and characterization of the human double-stranded RNA-activated protein kinase induced by interferon. Cell 62: 379–390.

Morita S, Villalta SA, Feldman HC, Register AC, Rosenthal W, Hoffmann-Petersen IT et al (2017) Targeting ABL-IRE1alpha signaling spares ER stressed pancreatic beta cells to reverse autoimmune diabetes. *Cell Metab.* 25, 883-897 e888.

Muniozguren NL, Zappa F & Acosta-Alvear D (2022) The integrated stress response induces a common cell-autonomous death receptor 5-dependent apoptosis switch. bioRxiv 2022.07.04.498696; doi: https://doi.org/10.1101/2022.07.04.498696.

Nadanaka S, Okada T, Yoshida H, & Mori K (2007) Role of Disulfide Bridges Formed in the Luminal Domain of ATF6 in Sensing Endoplasmic Reticulum Stress. Molecular and Cellular Biology 27, 1027-1043.

Nguyen Q & Yokota T (2019) Antisense oligonucleotides for the treatment of cardiomyopathy in Duchenne muscular dystrophy. Am J Transl Res 11: 1202–1218.

Nishitoh H, Matsuzawa A, Tobiume K, Saegusa K, Takeda K, Inoue K, Hori S, Kakizuka A & Ichijo H (2002) ASK1 is essential for endoplasmic reticulum stress-induced neuronal cell death triggered by expanded polyglutamine repeats. Genes Dev. 16(11):1345-55. doi: 10.1101/gad.992302. PMID: 12050113; PMCID: PMC186318.

Novoa I, Zhang Y, Zeng H, Jungreis R, Harding HP & Ron D (2003) Stress-induced gene expression requires programmed recovery from translational repression. EMBO J 22: 1180–1187.

Oslowski CM & Urano F (2011) Measuring ER stress and the unfolded protein response using mammalian tissue culture system. Methods Enzymol 490: 71–92.

Pakos-Zebrucka K, Koryga I, Mnich K, Ljujic M, Samali A & Gorman A (2016) The integrated stress response. EMBO reports. 17. 10.15252/embr.201642195.

Pichlmair A, Schulz O, Tan CP, Rehwinkel J, Kato H, Takeuchi O, Akira S, Way M, Schiavo G & Sousa C (2009) Activation of MDA5 Requires Higher-Order RNA Structures Generated during Virus Infection. Journal of virology. 83. 10761-9. 10.1128/JVI.00770-09.

Rafie-Kolpin M, Chefalo PJ, Hussain Z, Hahn J, Uma S, Matts RL & Chen JJ (2000) Two hene-binding domains of heme-regulated eukaryotic initiation factor-1alpha kinase. N terminus and kinase insertion. J Biold Chem 275: 5171-5178.

Ramirez M, Wek RC & Hinnebusch AG (1991) Ribosome association of GCN2 protein kinase, a translational activator of the GCN4 gene of Saccharomyces cerevisiae. Mol Cell Biol. (6):3027-36. doi: 10.1128/mcb.11.6.3027-3036.1991. PMID: 2038314; PMCID: PMC360137.

Relizani K & Goyenvalle A (2018) The Use of Antisense Oligonucleotides for the Treatment of Duchenne Muscular Dystrophy. Methods Mol Biol 1687: 171–183.

Reverendo M, Mendes A, Argüello RJ, Gatti E & Pierre P (2019) At the crossway of ER-stress and proinflammatory responses. FEBS J. 286(2):297-310. doi: 10.1111/febs.14391. Epub 2018 Feb 6. PMID: 29360216.

Rutkowski DT & Hegde RM (2010) Regulation of basal cellular physiology by the homeostatic unfolded protein response. *J Cell Biol* 31 May 2010; 189 (5): 783–794.

Sadler, A.J., & B.R.G. Williams (2007) Structure and function of the protein kinase R. Curr Top Microbiol Immunol. 316:253–292. doi:10.1007/978-3-540-71329-6_13.

Schoof M, Boone M, Wang L, Lawrence R, Frost A & Walter P (2021) eIF2B conformation and assembly state regulate the integrated stress response. eLife 10: e65703.

Schröder M (2008) Endoplasmic reticulum stress responses. Cell Mol Life Sci 65: 862–894.

Screaton GR, Mongkolsapaya J, Xu XN, Cowper AE, McMichael AJ & Bell JI (1997) TRICK2, a new alternatively spliced receptor that transduces the cytotoxic signal from TRAIL. Curr Biol 7: 693–696.

Siddiqui MA, Mukherjee S, Manivannan P & Malathi K (2015) RNase L Cleavage Products Promote Switch from Autophagy to Apoptosis by Caspase-Mediated Cleavage of Beclin-1. Int J Mol Sci 16:17611–17636.

Sidrauski C & Walter P (1997) The transmembrane kinase Ire1p is a site-specific endonuclease that initiates mRNA splicing in the unfolded protein response Cell 90, 1031-1039. Soi: 10.1016/S0092-8674(00)80369-4.

Sidrauski C, Acosta-Alvear D, Khoutorsky A, Vedantham P, Hearn BR, Li H, Gamache K, Gallagher CM, Ang KK-H, Wilson C, et al. (2013) Pharmacological brake-release of mRNA translation enhances cognitive memory. eLife 2: e00498.

Sidrauski C, McGeachy AM, Ingolia NT & Walter P (2015) The small molecule ISRIB reverses the effects of eIF2α phosphorylation on translation and stress granule assembly. eLife 4: e05033.

Taniuchi S, Miyake M, Tsugawa K, Oyadomari M & Oyadomari S (2016) Integrated stress response of vertebrates is regulated by four eIF2α kinases. Sci Rep. 6:32886. doi: 10.1038/srep32886. PMID: 27633668; PMCID: PMC5025754.

Tian X, Zhang S, Zhou L, Seyhan AA, Hernandez Borrero L, Zhang Y & El-Deiry WS (2021) Targeting the Integrated Stress Response in Cancer Therapy. Front. in Pharmacol, 12. doi:10.3389/fphar.2021.747837.

Urano F, Wang X, Bertolotti A, Zhang Y, Chung P, Harding HP & Ron D (2000) Coupling of stress in the ER to activation of JNK protein kinases by transmembrane protein kinase IRE1. Science. 287(5453):664-6. doi: 10.1126/science.287.5453.664. PMID: 10650002.

Valley CC, Lewis AK, Mudaliar DJ, Perlmutter JD, Braun AR, Karim CB, Thomas DD, Brody JR & Sachs JN (2012) Tumor necrosis factor-related apoptosis-inducing ligand (TRAIL) induces death receptor 5 networks that are highly organized. J Biol Chem 287: 21265–21278.

Vattem KM, Staschke KA & Wek RC (2001) Mechanism of activation of the double-stranded- RNA-dependent protein kinase, PKR: role of dimerization and cellular localization in the stimulus of PKR phosphorylation of eukaryotic initiation factor 2 (eIf2) Eur. J. Biochem, 268, pp. 3674-3684.

Vattem KM & Wek RC (2004) Reinitiation involving upstream ORFs regulates ATF4 mRNA translation in mammalian cells. Proc Natl Acad Sci U S A 101: 11269–11274.

Vazquez de Aldana CR, Wek RC, Segundo PS, Truesdell AG & Hinnebusch AG (1994) Multicopy tRNA genes functionally suppress mutations in yeast eIF 2 alpha kinase GCN2 evidence for separate pathways coupling GCN4 expression to unchanged tRNA. Mol Cell Biol 14: 7920-7932.

Walter P & Ron D (2011) The Unfolded Protein Response: From Stress Pathway to Homeostatic Regulation. Science 334, 1081-1086.

Wang P, Li J, Tao J & Sha B (2018) The luminal domain of the ER stress sensor protein PERK binds misfolded proteins and thereby triggers PERK oligomerization. J Biol Chem 293: 4110–4121.

Williams BR (1999) PKR; a sentinel kinase for cellular stress. Oncogene. Nov 1;18(45):6112-20. doi: 10.1038/sj.onc.1203127. PMID: 10557102.

Wilson NS, Dixit V & Ashkenazi A (2009) Death receptor signal transducers: nodes of coordination in immune signaling networks. Nat Immunol 10: 348–355.

Wiseman RL, Zhang Y, Lee KP, Harding HP, Haynes CM, Price J, Sicheri Fb& Ron D (2010) Flavonol activation defines an unanticipated ligand-binding site in the kinase-RNase domain of IRE1. Mol Cell 38(2):291-304. doi: 10.1016/j.molcel.2010.04.001. PMID: 20417606; PMCID: PMC2864793.

Wood MJA, Talbot K & Bowerman M (2017) Spinal muscular atrophy: antisense oligonucleotide therapy opens the door to an integrated therapeutic landscape. Hum Mol Genet 26: R151–R159.

Wu S & Kaufman RJ (1997) A model for the double-stranded RNa (dsRNA)-dependent dimerization and activation of the dsRNA-activates protein kinase PKR. J. Biol. Chem, 272, pp.1291-1296.

Wu S, Hu Y, Wang JL, Chatterjee M, Shi Y & Kaufman RJ (2002) Ultraviolet light inhibits translation through activation of the unfolded protein response kinase PERK

in the lumen of the endoplasmic reticulum. J Biol Chem. 277(20):18077-83. doi: 10.1074/jbc.M110164200. Epub 2002 Mar 4. PMID: 11877419.

Wu CC-C, Peterson A, Zinshteyn B, Regot S & Green R (2020) Ribosome Collisions Trigger General Stress Responses to Regulate Cell Fate. Cell 182: 404–416.e14.

Yamaguchi H & Wang H-G (2004) CHOP is involved in endoplasmic reticulum stress-induced apoptosis by enhancing DR5 expression in human carcinoma cells. J Biol Chem 279: 45495–45502.

Yamamoto K, Ichijo H & Korsmever SJ (1999) BCL-2 is phosphorylated and inactivated by an ASK1/Jun N-terminal protein kinase pathway normally activates at G(2)/M. Mol. Cell. Biol. 19:8469-8478.

Yamamoto K, Yoshida H, Kokame K, Kaufman RJ & Mori K (2004) Differential contributions of ATF6 and XBP1 to the activation of endoplasmic reticulum stress-responsive cis-acting elements ERSE, UPRE and ERSE-II. J Biochem. 136(3):343-50. doi: 10.1093/jb/mvh122. PMID: 15598891.

Yang W, Rozamus LW, Narula S, Rollins CT, Yuan R, Andrade LJ, Ram M0K, Phillips TB, van Schravendijk MR, Dalgarno D, Clackson T & Holt DA (2000) Investigating Protein−Ligand Interactions with a Mutant FKBP Possessing a Designed Specificity Pocket. J. Med. Chem. 43:1135–1142. doi:10.1021/jm9904396.

Ye J, Rawson RB, Komuro R, Chen X, Davé UP, Prywes R, Brown MS, & Goldstein JL (2000) ER Stress Induces Cleavage of Membrane-Bound ATF6 by the Same Proteases that Process SREBPs. Molecular Cell 6, 1355-1364.

Yerlikaya A, Kimball SR & Stanley BA (2008) Phosphorylation of EIF2alpha in response to 26S proteosome inhibition is mediated by heme-regulated inhibitor (HRI) kinase. Biochem J 412: 579-588.

Zappa F, Muniozguren NL, Wilson MZ, Costello MS, Ponce-Rojas JC & Acosta-Alvear D (2022) Signaling by the integrated stress response kinase PKR is fine-tuned by dynamic clustering. Journal of Cell Biology 221: e202111100.

Zhou Z-x, Zhang B-c & Sun L (2014) Poly(I:C) Induces Antiviral Immune Responses in Japanese Flounder (*Paralichthys olivaceus*) That Require TLR3 and MDA5 and Is Negatively Regulated by Myd88. PLoS ONE 9(11): e112918. https://doi.org/10.1371/journal.pone.0112918.

Zhu PJ, Khatiwada S, Cui Y, Reineke LC, Dooling SW, Kim JJ, Li W, Walter P & Costa-Mattioli M (2019) Activation of the ISR mediates the behavioral and neurophysiological abnormalities in Down syndrome. Science 366: 843–849.

Zhu Z, Liu P, Yuan L, Lian Z, Hu D, Yao X & Li X (2021) Induction of UPR Promotes Interferon Response to Inhibit PRRSV Replication *via* PKR and NF-κB Pathway. Front Microbiol. 12:757690. doi: 10.3389/fmicb.2021.757690. PMID: 34712218; PMCID: PMC8547762.